DOI: 10.1002/ejic.201000948

# Vanadium(IV) and -(V) Complexes of Reduced Schiff Bases Derived from Aromatic *o*-Hydroxyaldehydes and Tyrosine Derivatives

**Isabel Correia,*[a] Susana Marcão,[a] Kamila Koci,[a][‡] Isabel Tomaz,[a][‡‡] Pedro Adão,[a] Tamás Kiss,*[b] Tamás Jakusch,[c] Fernando Avecilla,[d] and João Costa Pessoa*[a]**

**Keywords:** N,O ligands / Vanadium / Structure elucidation / Coordination modes / Potentiometry

The reduced Schiff bases of salicylaldehyde and pyridoxal (and *o*-vaniline) with L-tyrosine (Tyr) and D,L-*o*-tyrosine (*o*-Tyr), designated as sal-Tyr (**1**), sal-*o*-Tyr (**2**), pyr-Tyr (**3**), pyr-*o*-Tyr (**4**), and *o*-van-L-Tyr (**5**), as well as the oxidovanadium(IV) complex VO(sal-*o*-Tyr) (**6**) have been prepared. The compounds have been characterized in the solid state and in solution. The structure of **3** has been determined by X-ray diffraction. Complexation of these ligands with vanadium in aqueous solution has been studied by pH potentiometry, UV/Vis, and circular dichroism (for the L-Tyr derivatives), as well as by EPR for the $V^{IV}O$ systems and $^{51}V$ NMR for the $V^{V}O_2$ systems. Stoichiometries and complex formation constants have been determined by pH potentiometry (25 °C, $I$ = 0.2 M KCl) 1:1 complexes are formed in most systems with variable protonation states $VOLH_2$ (only with **3** and **4**), VOLH, VOL, and $VOLH_{-1}$. Dinuclear species $(VOL)_2H$ and $(VOL)_2$ were identified only in the case of **3**. Spectroscopic data provided information about the most probable binding modes for each stoichiometry. The $V^{IV}O$ complexes formed with the *o*-Tyr-derived ligands are more stable than those with L-Tyr, the more adequate coordination position of the phenolate in the *o*-Tyr ligands shows a more significant stabilizing effect compared with **3** and **4**.

## Introduction

The presence of vanadium in biological systems, its presence in vanadium-dependent haloperoxidases[1] and nitrogenases,[2] its possible physiological roles,[3] its insulin-enhancing action,[4–10] and anticancer activity[11–14] have driven a considerable amount of research. Particular attention has been paid to the study of the potential benefits of vanadium compounds as oral insulin substitutes for the treatment of diabetes. Coordinated ligands should be able to improve the absorption and possibly the transport and uptake of vanadium into the cells, reducing the dose necessary for efficacy and lowering metal ion toxicity.

[a] Centro Química Estrutural, Instituto Superior Técnico, TU Lisbon,
Av. Rovisco Pais, 1049-001 Lisboa, Portugal
[b] Department of Inorganic and Analytical Chemistry University of Szeged,
P. O. Box 440, 6701 Szeged, Hungary
[c] Bioinorganic Chemistry Research Group of the Hungarian Academy of Sciences, Department of Inorganic and Analytical Chemistry, University of Szeged,
P. O. Box 440, 6701 Szeged, Hungary
[d] Departamento de Química Fundamental, Universidaded de Coruña,
Campus de A Zapateira s/n, 15071 A Coruña, Spain
[‡] Present address: Mass Spectrometry Laboratory, ITQB – UNL,
Av. República, EAN,
Apartado 127, 2781-901 Oeiras, Portugal
[‡‡] Present address: Centro de Ciências Moleculares e Materiais, Faculdade de Ciências da Universidade de Lisboa,
Ed. C8, Campo Grande, Campo Grande, 1749-016 Lisboa, Portugal

Supporting information for this article is available on the WWW under http://dx.doi.org/10.1002/ejic.201000948.

The mechanisms by which vanadium compounds mediate antidiabetic effects in vivo are poorly described and understood. It is known that vanadate is a very potent inhibitor for phosphatases and other phosphorylases,[3,15] and key events appear to involve inhibition of protein tyrosine phosphatases and tyrosine kinases.[3,16–18] Several vanadium complexes have been found to have better insulin enhancing activities than inorganic vanadate(V) or oxidovanadium(IV) salts, but most likely this improved efficacy relates to bioavailability rather than to increased potency at the phosphatase enzyme active sites.[16]

The binding of $V^{IV}O^{2+}$ and vanadate to the tyrosine residues at the C- and N-terminal ends of transferrin is well documented,[19–23] as well as the direct binding of vanadate to tyrosine in tyrosyl-DNA phosphodiesterase.[24] However, the amino acid itself is quite ineffective in coordination to vanadium. Dipeptides containing Tyr are more effective binders but the main complexes exclude Tyr from direct binding.[25] The presence of an anchor group in the ligand may enhance the binding ability of the ligand. In this sense *N*-salicylidene amino acidato-type complexes have been extensively studied[26–30] and, in many cases, they may be easily prepared by the condensation of an aromatic *o*-hydroxyaldehyde and an amino acid. However, these Schiff bases (SBs) may hydrolyse in solution, and in many cases it is not possible to characterize either the ligands or their complexes in the solid state. This instability can sometimes be overcome by reduction of the SB at the imine function to give an amine.[31–35] A few reduced SBs of salicylaldehyde

  

with amino acids have been isolated,[32,33] and their [$V^{V}$OL(hq)] complexes (Hhq = 8-hydroxyquinoline) prepared and characterized.[33]

Most of the biologically important reactions of vanadium occur in water-based environments such as blood plasma or other physiological fluids and intracellular media. Therefore the knowledge of the distribution and chemical speciation of vanadium compounds in aqueous solution is of utmost importance. We report the preparation of the reduced SBs of salicylaldehyde and pyridoxal (and *o*-vanillin) with L-Tyr and D,L-*o*-tyrosine. Compounds sal-Tyr (**1**), sal-*o*-Tyr (**2**), pyr-Tyr (**3**), pyr-*o*-Tyr (**4**), and *o*-van-L-Tyr (**5**) have been prepared (their molecular formulae are depicted in Scheme 1) and are characterized in the solid state and in solution. Their complex formation with $V^{IV}O^{2+}$ and $V^{V}O_2^{+}$ in aqueous solution in the pH range 2–11 is also studied by potentiometric and spectroscopic methods (except **5**). For comparison a few solution studies with the amino acid D,L-*o*-tyrosine are also presented.

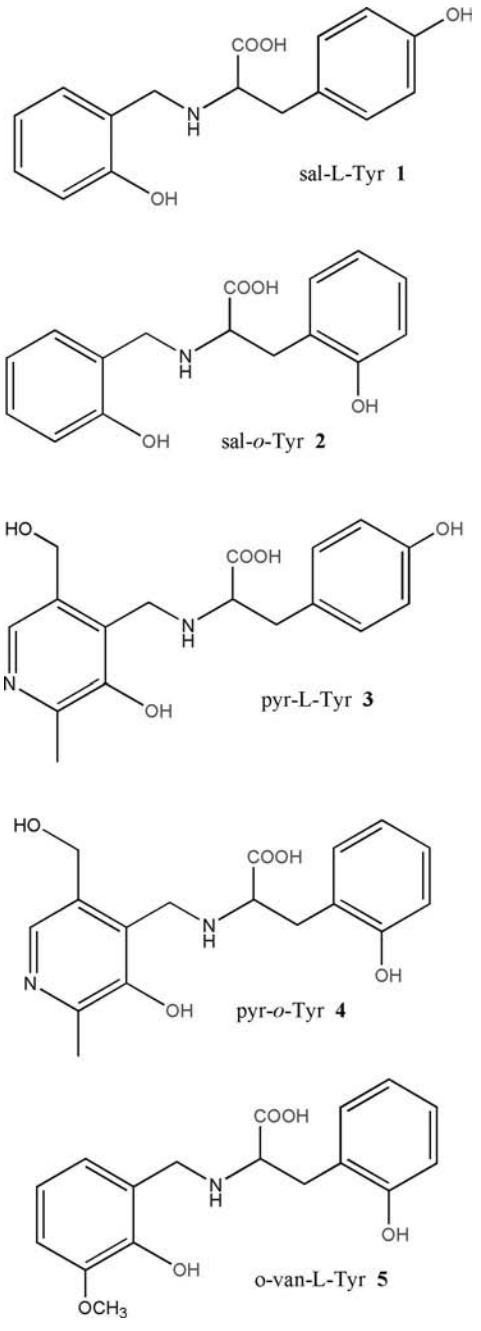


Scheme 1. Molecular formulae of the four reduced SB compounds prepared. The totally protonated compounds **1**, **2**, and **5** correspond to $H_4L^+$, and **3** and **4** to $H_5L^{2+}$ and by the main procedure used were obtained in the solid state in the zwitterionic form. For compound **5** a different synthetic procedure was used and it was obtained in its protonated form $H_4L^{+}\cdot Cl^{-}$, with protons at the amine and carboxylic groups. Its protonation/deprotonation properties were not studied. When designating these compounds without specific attention to their protonation state, we will omit the protonation state. Note that in this work Tyr corresponds to L-Tyr and *o*-Tyr to the racemic mixture D,L-*o*-Tyr.

## Results and Discussion

### Synthesis and Characterisation

The reduced SBs **1**–**5**, depicted in Scheme 1, were prepared by the condensation of one equivalent of the appropriate aldehyde with one equivalent of amino acid. Treatment of these condensation products with sodium borohydride resulted in the reduction of the imine bonds, yielding the reduced SBs. The compounds were characterised by the usual spectroscopic techniques, mass spectrometry, and elemental analysis.

Crystals of **3** suitable for X-ray diffraction studies were obtained and details on the crystal structure are given in the Supporting Information (SI). An ORTEP diagram with the molecular structure is depicted in Figure 1. The L-Tyr moiety is present in the zwitterionic form with the amine nitrogen atom protonated and the carboxylate group deprotonated. It is interesting to note that in the pyridoxal moiety the phenolate atom O(2) is deprotonated and the pyridinic

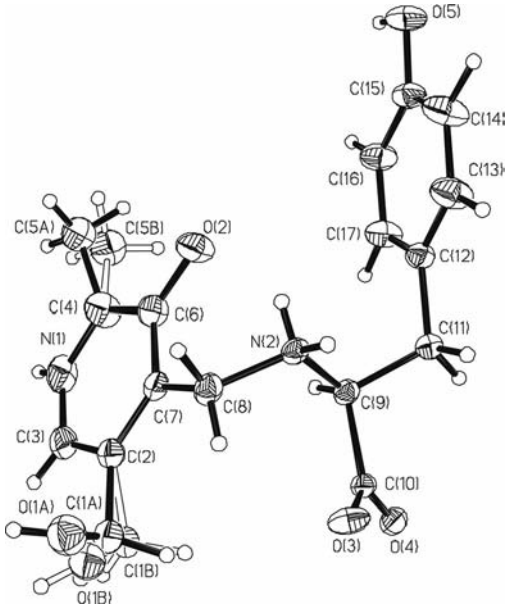


Figure 1. ORTEP diagram of **3** with thermal ellipsoids of the non-hydrogen atoms drawn at 30% probability level.

  

atom N(1) is protonated. The bond lengths found for **3** are within the expected ranges and selected bond lengths and angles are included in Table 1. In SBs the C=N distances are typically 1.24–1.28 Å,[26–31] and the C(8)–N(2) and C(9)–N(2) bond lengths of 1.498(3) and 1.493(3) Å, respectively, are consistent with the formation of single bonds.[31,34,37]

Table 1. Selected bond lengths [Å] and angles (°) for **3**.

| Bond lengths (Å) | | Angles (°) | |
|---|---|---|---|
| N(1)–C(3) | 1.319(4) | C(3)–N(1)–C(4) | 124.8(2) |
| N(1)–C(4) | 1.342(3) | O(1A)–C(1A)–C(2) | 116.3(5) |
| O(1A)–C(1A) | 1.394(8) | O(1B)–C(1B)–C(2) | 107.3(9) |
| C(1A)–C(2) | 1.546(7) | C(9)–N(2)–C(8) | 117.59(17) |
| O(1B)–C(1B) | 1.329(12) | C(3)–C(2)–C(1B) | 113.7(8) |
| C(1B)–C(2) | 1.456(13) | C(7)–C(2)–C(1B) | 126.1(9) |
| N(2)–C(9) | 1.493(3) | C(3)–C(2)–C(1A) | 122.1(5) |
| N(2)–C(8) | 1.498(3) | C(7)–C(2)–C(1A) | 119.0(5) |
| O(2)–C(6) | 1.287(3) | N(1)–C(3)–C(2) | 120.0(2) |
| O(3)–C(10) | 1.234(3) | N(1)–C(4)–C(6) | 118.8(2) |
| O(4)–C(10) | 1.264(3) | N(1)–C(4)–C(5B) | 118.0(3) |
| C(4)–C(5B) | 1.492(7) | C(6)–C(4)–C(5B) | 122.0(3) |
| C(4)–C(5A) | 1.541(7) | N(1)–C(4)–C(5A) | 117.7(3) |
| O(5)–C(15) | 1.373(3) | C(6)–C(4)–C(5A) | 121.1(3) |
| | | O(2)–C(6)–C(7) | 121.5(2) |
| | | O(2)–C(6)–C(4) | 121.9(2) |
| | | N(2)–C(8)–C(7) | 111.99(18) |
| | | N(2)–C(9)–C(10) | 113.01(16) |
| | | N(2)–C(9)–C(11) | 108.33(17) |
| | | O(3)–C(10)–O(4) | 125.76(19) |
| | | O(3)–C(10)–C(9) | 119.15(19) |
| | | O(4)–C(10)–C(9) | 115.04(18) |

The configuration of **3** is determined by medium/strong intramolecular and intermolecular H-bonds: the –NH groups of the pyridoxyl rings are involved in an intermolecular hydrogen bond with the oxygen atom O(3) of a carboxylate group. The disordered $–CH_2OH$ groups are involved in an intermolecular H-bond with the phenolate O(2). The $–NH_2$ groups present two types of H-bonds, intermolecular and intramolecular, with the oxygen atoms O(4) of the carboxylate group and O(2) of the phenolate, respectively. The oxygen atoms O(5) of the phenolic rings are involved in an intermolecular H-bond with the carboxylate group O(4).

The only neat $V^{IV}O$ complex characterized in the solid state is $V^{IV}O$(sal-*o*-Tyr) (**6**). Although vanadium-containing complexes were isolated for the other systems, no satisfactory formulation was found for these solids. Some selected IR data for the ligands and vanadium complex are shown in the Supporting Information. All compounds present broad bands in the range 2400–3500 $cm^{-1}$ corresponding to H-bonded (symmetrical and antisymmetrical) O–H, N–H and overtone bands.[38] For all ligands sharp bands emerge from this broad band, assigned to ν(N–H). The $\nu_{as}$(COO) appear at 1615–1650 $cm^{-1}$, whereas the $\nu_s$(COO) are assigned to the bands observed at 1456–1464 $cm^{-1}$. No bands are observed in the range 1640–1750 $cm^{-1}$ indicating the zwitterionic nature of compounds **1**–**4**. The strong bands at 1250–1270 $cm^{-1}$ are assigned to the $\nu(C–O_{phenolate})$. In the IR spectrum of solid **6** the characteristic ν(V=O) appears as a strong band at 957 $cm^{-1}$, suggesting a square pyramidal structure in the solid state possibly with apical interactions between neighbouring molecules that decrease the strength of the V=O bond.[39]

## Solution Studies

The protonation constants for the ligands and formation constants for their $V^{IV}O$ complexes are defined according to Equation (1), where charges are omitted for the products for simplicity [Equation (1)].

$$p\ V^{IV}O^{2+} + q\ L^{3-} + r\ H^{+} \leftrightarrows (V^{IV}O)_p(L)_q(H)_r \quad (1)$$

A similar expression is valid for $V^{V}O_2$ complexes: $(V^{V}O_2)_p(L)_q(H)_r$. In the particular case of the protonation constants of ligands, the stoichiometric index $p$ is equal to zero and the species are represented as $H_rL$ instead of $LH_r$. The complexes corresponding to stoichiometries $(V^{IV}O)_p(L)_q(H)_r$ and $(V^{V}O_2)_p(L)_q(H)_r$ are written as $(V^{IV}O)_pL_qH_r$ and $(V^{V}O_2)_pL_qH_r$, respectively.

## Ligands

Compounds **1**–**4** are stable in solution in a wide pH range. Protonation constants and $pK_a$ values obtained from pH potentiometric titrations are listed in Table 2. The values for D,L-*o*-Tyr determined by pH potentiometry are also included for comparison. The fully protonated compounds **1** and **2** correspond to $H_4L^+$, **3** and **4** to $H_5L^{2+}$ and D,L-*o*-Tyr and L-Tyr to $H_3L^+$. The $pK_a$ of the carboxylic group is relatively low, nevertheless it was determined by pH metric measurements for all ligands and spectophotometric titrations confirmed these values. UV spectra and details on the calculations are included in the Supporting Information.

pH Potentiometry alone does not provide information on the sequence of protonation. The assignment of each protonation step to each basic group may be done through the pH dependency of the chemical shift ($\delta$) of the neighbouring atoms of the ionisable groups. $^1$H NMR titration studies [$\delta$ (ppm) vs. pH] were carried out for **1**–**4** in $D_2O$. Compounds **1** and **2** precipitated in the pH range 4–9, and only limited information was obtained for these two ligands. Figure 2 depicts the titration curves obtained for **4** (ligand **3** is included in the Supporting Information), and the assignment of the proton peaks. The protonation sequence can be deduced from the relative values of the protonation shifts and by comparison with studies reported for related compounds, however, the existence of microequilibria and/or isomers with same stoichiometry but protonated at different sites cannot be excluded.

The highest $pK_a$ value for ligands **1**–**4** is above 10, and, by comparison with D,L-*o*-Tyr, can be assigned to the phenolic OH group of the Tyr side chain. This is consistent with the highest $\Delta\delta$ observed for the aromatic protons of the Tyr side chain, which is between pH 9 and 12. The aromatic proton in the pyridinic ring H(10) is expected to be sensitive

  

Table 2. Protonation constants for the ligands and formation constants for the $V^{IV}O$ and $V^{V}O_2$ complexes, as defined in Equation 1, calculated with the PSEQUAD computer program;[57] $T$ = 25 °C and $I$ = 0.2 M KCl. The charges of the species are omitted.

| Stoichiometry | D,L-*o*-Tyr | | sal-L-Tyr (**1**) | | sal-*o*-Tyr (**2**) | | pyr-L-Tyr (**3**) | | pyr-*o*-Tyr (**4**) | |
|---|---|---|---|---|---|---|---|---|---|---|
| | $\log\beta_{pqr}$ | $pK_a$ | $\log\beta_{pqr}$ | $pK_a$ | $\log\beta_{pqr}$ | $pK_a$ | $\log\beta_{pqr}$ | p*K*a | $\log\beta_{pqr}$ | $pK_a$ |
| **Ligands** | | | | | | | | | | |
| HL | 10.96(5) | 10.96 | 10.93(5) | 10.93 | 12.32(27) | 12.32 | 10.50(3) | 10.50 | 11.80(7) | 11.80 |
| $H_2L$ | 19.56(7) | 8.59 | 20.69(7) | 9.76 | 22.06(9) | 9.75 | 20.15(3) | 9.65 | 21.12(10) | 9.32 |
| $H_3L$ | 21.81(7) | 2.25 | 28.79(8) | 8.10 | 30.08(10) | 8.02 | 27.82(4) | 7.67 | 28.80(10) | 7.68 |
| $H_4L$ | | | 30.51(10) | 1.72[a] | 32.19(10) | 2.12[a] | 30.92(6) | 3.10 | 31.99(11) | 3.19 |
| $H_5L$ | | | | | | | 32.53(9) | 1.61[a] | 33.47(12) | 1.49 [a] |
| **$V^{IV}$ Complexes** | | | | | | | | | | |
| $VOLH_2$ | 21.31(17) | 4.17 | – | | | | 29.50(2) | 6.46 | 30.74(2) | 5.13 |
| VOLH | 17.14(16) | | 23.54(5) | 7.11 | 24.73(3) | 6.06 | 23.04(5) | | 25.61(4) | 7.27 |
| VOL | – | | 16.43(9) | 9.3 | 18.67(7)[b] | 9.23 | – | | 18.34(5) | 9.48 |
| $VOLH_{-1}$ | – | | 7.1(3) | | 9.44(24) | | – | | 8.86(7) | |
| $(VO)_2L_2H$ | | | | | | | 41.89(10) | 8.50 | | |
| $(VO)_2L_2$ | | | | | | | 33.39(26) | | | |
| **$V^{V}$ Complexes** | | | | | | | | | | |
| $VO_2LH_2$ | | | | | | | | | 31.41(4) | 5.93 |
| $VO_2LH$ | | | | | | | | | 25.48(5) | 7.84 |
| $VO_2L$ | | | | | | | | | 17.64(6) | |

[a] These $pK_a$ values were confirmed by spectrophotometric titrations (range ca. $200 < \lambda < 360$ nm), which gave the following values: $1.75 \pm 0.02$ (**1**); $2.10 \pm 0.11$ (**2**); $1.57 \pm 0.02$ (**3**); $1.51 \pm 0.02$ (**4**). [b] When VOL was not included in the equilibrium model the dinuclear species $(VO)_2L_2$ was refined with a $\log\beta = 35.87 \pm 0.06$, but the fitting parameter was much worse. When both species were included, $(VO)_2L_2$ was rejected. This dinuclear species was also rejected in the refinement of the speciation model of the VO–**1** system.

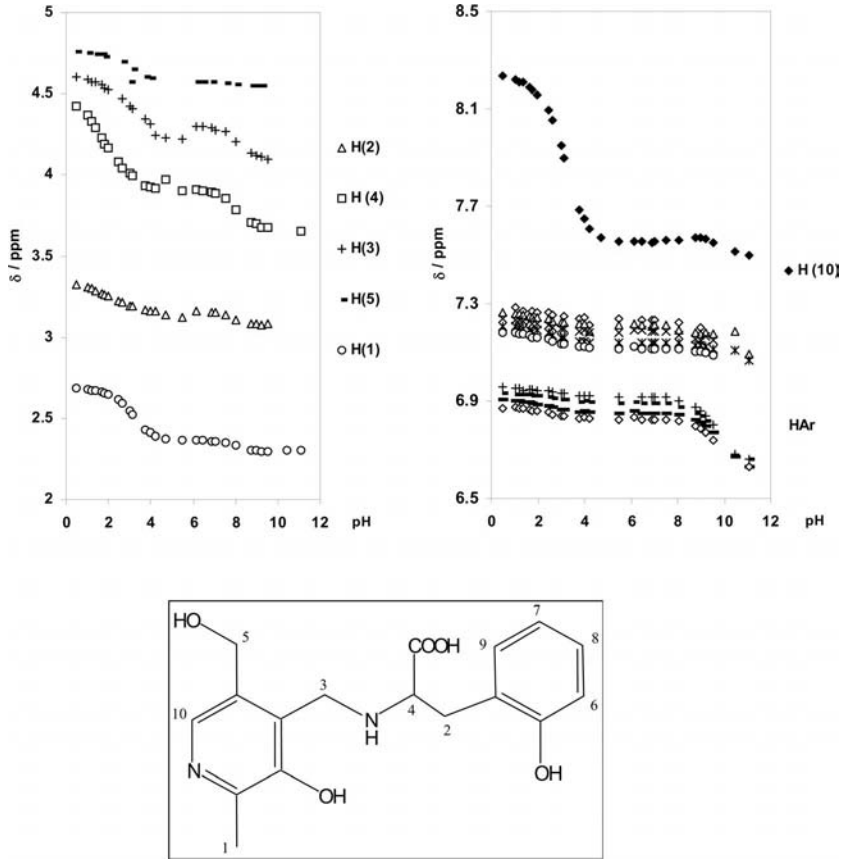


Figure 2. $^1$H NMR titration of **4** and labelling of the peaks. The aromatic protons H(6), H(7), H(8), and H(9) appear as doublets, and are assigned in the Figure as HAr.

to the protonation of the adjacent $N_{pyridine}$ group. The major shift in $\delta$ for this proton is observed between $2 < pH < 4$, and the protonation of this group can be assigned to the second $pK_a$ value (ca. 3.1). This is also suggested by the $\Delta\delta$ observed for H(1) in this pH region ($\delta$ = 0.23 ppm), however, as the $O_{phenolate}$ is connected to the

  

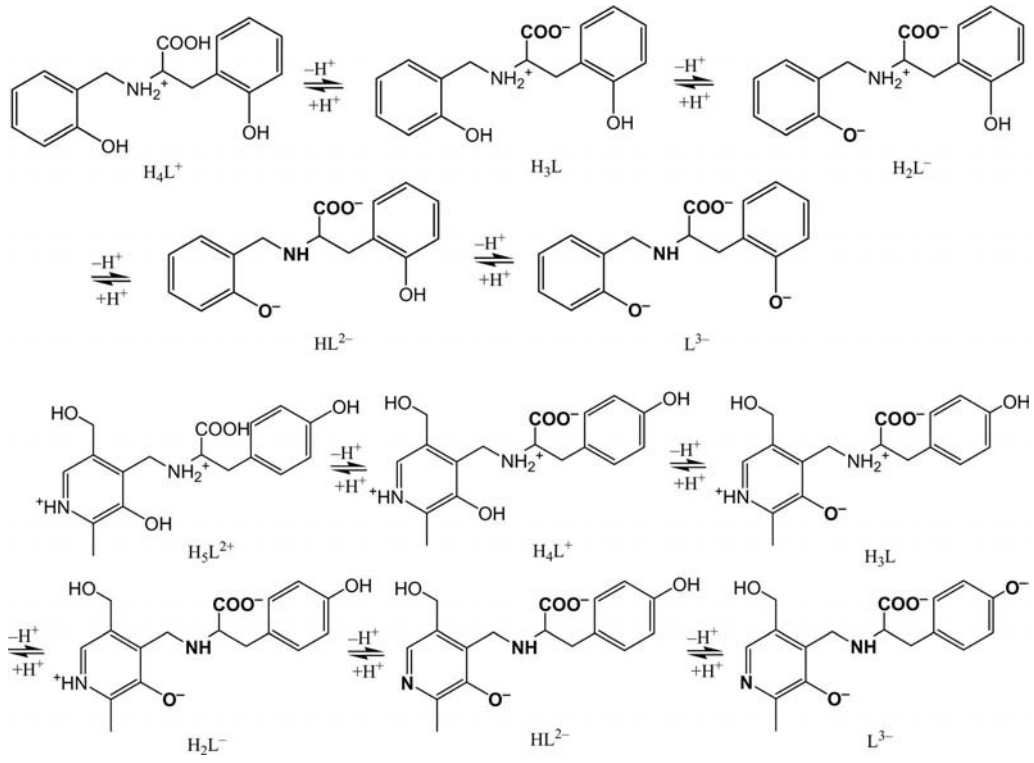


Scheme 2. Deprotonation sequence proposed for ligands **2** (above) and **4** (below).

aromatic ring, its protonation may have the same effect. The crystal structure of the ligand suggests that the deprotonation of the phenolate group occurs first. Moreover, earlier studies with pyridoxal derivatives showed the same deprotonation order.[31,41]

To assign the p$K_a$ to the $N_{amine}$ and $N_{pyridine}$ protonations we can analyse the behavior of protons H(4) and H(3) near the $N_{amine}$ group. Proton H(4) shows high $\Delta\delta$ between $1 < pH < 4$ and $7 < pH < 9$; H(3) also shows a considerable shift between pH 6.0 and 9.0. Thus, we can tentatively assign the p$K_a$ value of 7.68 to the deprotonation of the $N_{amine}$ group and accordingly the p$K_a$ of 9.67 is assigned to the $N_{pyridine}$.

Taking into account the analysis of the NMR titration data for **3**, we propose the following protonation sequence for both ligands: $COO^-$, $O_{phenolate}$, $N_{amine}$, $N_{pyridinic}$, and the Tyr side chain $O_{phenolate}$, which is depicted in Scheme 2 for ligand **4**. Nevertheless, this protonation sequence cannot be simply extrapolated for **1** and **2** since the absence of the N atom and the aromatic substituents should not decrease the $O_{phenolate}$ p$K_a$ value that much. For **1** and **2** it is reasonable to accept that the carboxylic moiety deprotonates first and the side chain phenolic OH group last. The possibility of H bond formation between $O_{phenolate}$ and $N_{amine}$ makes the discussion of the order of deprotonation between these groups almost meaningless. Analysis of the statistical data shows a low standard error for all p$K_a$ values except for the side chain $O_{phenolate}$. This is due to the higher value determined for this p$K_a$ in **2**. The possibility of H- bonding between the phenolate oxygen in *ortho* position and the deprotonated carboxylate or the NH group must be responsible for the higher basicity of both groups in this compound.

## $V^{IV}O$ Complexes

Compounds **1**–**4** are able to coordinate to $V^{IV}$, and complex formation was monitored using potentiometry and spectroscopy (UV/Vis, CD and EPR). Although slow equilibration or precipitation of $V^{IV}O(OH)_2$ occurred in some cases for $pH > 4$, carefully chosen experimental titration conditions varying the total oxidovanadium(IV) concentration and ligand to metal ratios (L:M) allowed the solution characterization of all systems. The complex formation constants, defined by Equation (1), were calculated from potentiometric titrations carried out at different vanadium/ligand ratios and are included in Table 2. Concentration distribution diagrams are presented in Figure 3.

Compound D,L-*o*-Tyr forms stable complexes with $V^{IV}O^{2+}$, with stoichiometries $VOLH_2$ and VOLH in the pH range 2–4, but the hydrolytic products of $V^{IV}O^{2+}$, namely $[(V^{IV}O)_2(OH)_2]^{2+}$, have a much higher relative importance in the pH range of formation of species VOLH in the $V^{IV}O$-*o*-Tyr system than for the other studied $V^{IV}O$ systems (see below). Thus, *o*-Tyr is a weak $V^{IV}O$ binder as when the L:M ratio is 2:1 or lower it is unable to prevent hydrolysis of the metal ion and precipitation of $VO(OH)_2$ at pH ≈ 4.5 (see Figure 3, e). Ligands **1**–**4** contain a suitable $O_{phenolate}$ donor

  

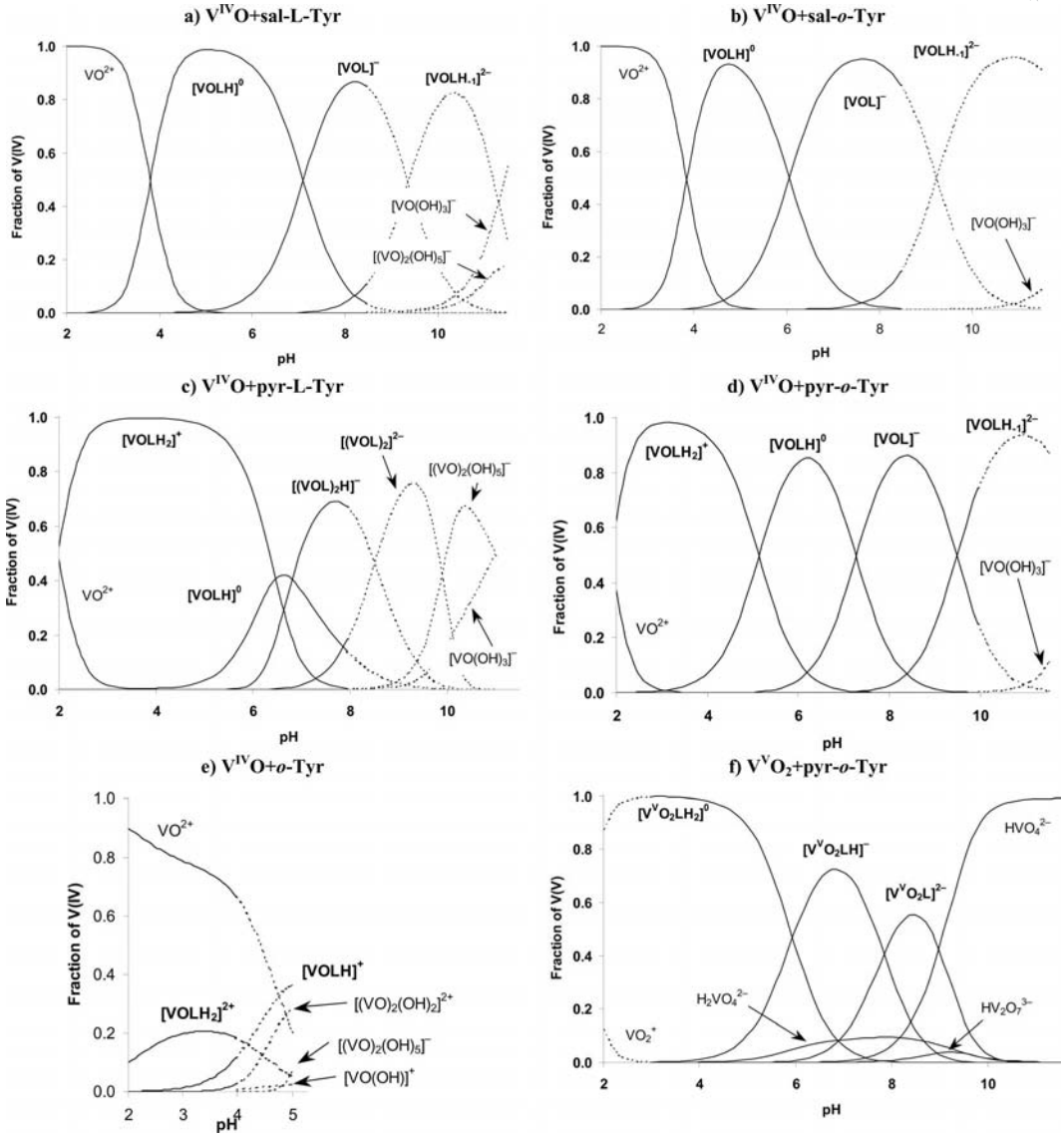


Figure 3. Concentration distribution diagrams for the vanadium-containing systems. Conditions: $C_{V^{IV}\text{ or }V^{V}}$ = 3 mM, L:M = 2:1, 25 °C and $I$ = 0.2 M KCl: a) $V^{IV}O^{2+}$ + **1**; b) $V^{IV}O^{2+}$ + **2**; c) $V^{IV}O^{2+}$ + **3**; d) $V^{IV}O^{2+}$ + **4**; e) $V^{IV}O^{2+}$ + *o*-Tyr, f) $V^{V}O_2^{+}$ + **4**. Dotted lines indicate the pH range where the model is less accurate (due to hydrolysis and/or slow equilibria). The $O_{phenolate}$ anchor from the aromatic aldehyde in ligands **1**–**4** can stabilize vanadium in solution being able to efficiently extend the binding ability of Tyr (**e**) to a wider pH range, especially if present in the *ortho* position (b, d, f).

which allows the formation of a (6+5) chelation system that can stabilize the metal ion in solution in a wider pH range.

The interaction of $V^{IV}O^{2+}$ with **1** results in the formation of the neutral species VOLH, which predominates between pH 4 and 7. Further successive deprotonations yield VOL (p$K_a$ = 7.11) and $VOLH_{-1}$ (p$K_a \approx$ 9.3). The same behavior and stoichiometries are observed in the $V^{IV}O$ system with **2**. The p$K_a$ values of the $V^{IV}O$ complexes with **1** and **2** differ in more than one pH unit and the proton displacement constants ($K$*) characteristic to the formation equilibrium: $V^{IV}O^{2+} + H_3L^{+} \leftrightarrows V^{IV}OL + 3H^{+}$ have the following log $K$* values: –12.36 and –11.41 for **1** and **2**, respectively. Therefore, **2**, with a Tyr-$O_{phenolate}$ donor atom in the *ortho* position, has higher affinity for $V^{IV}O$.

EPR spectra were measured in frozen solution (77 K) to confirm the speciation model and to elucidate the binding modes for the various stoichiometries. EPR spectra in the region corresponding to $M_I$ = 5/2 and 7/2 obtained for the $V^{IV}O$ systems are depicted in the Supporting Information. Table 3 shows the spin Hamiltonian parameters obtained by simulation of the experimental spectra.[40] Wüthrich[42] and Chasteen[43] developed an additivity rule to estimate the hyperfine coupling constant $A_z^{est}$ [$A_z^{est} = \Sigma A_{z,i}$ ($i$ = 1–4)] for $V^{IV}O$ systems based on the contributions $A_{z,i}$ of each of the four equatorial donor groups. The estimated accuracy of $A_z^{est}$ is $\pm 1.5 \times 10^{-4}$ cm$^{-1}$.

The $A_{z,i}$ values used in this work are as follows: $A_{z,COO^-} = 42.1 \times 10^{-4}$ cm$^{-1}$,[44] $A_{z,phenolate} = 38.9 \times 10^{-4}$, $A_{z,amine}$ =

  

Table 3. Spin Hamiltonian parameters obtained by simulation of the EPR spectra. Plausible binding modes are also indicated for each species formed. Hyperfine coupling constants ($A_z$, $A_\perp$) are given in $\times 10^4$ cm$^{-1}$. The $A_z^{est}$ presented do not take into account any influence from axially bound donors.[48]

| System and stoichiometry | $g_\perp$ | $g_z$ | $A_\perp$ | $A_z$ | $A_z^{est}$ | Binding modes ($O_{phe}$ = $O_{phenolate}$) |
|---|---|---|---|---|---|---|
| **VO–sal-Tyr** | | | | | | |
| II – VOL | 1.977 | 1.946 | 59.0 | 168.6 | 166.6 | $(N_{amine}, COO^-, OH_2, OH^-)_{eq}$ $(O^-_{phe})_{ax}$[b] |
| III – $VOLH_{-1}$ | 1.976 | 1.949 | 56.5 | 165.4 | 165.3 | $(O^-_{phe}, COO^-, OH_2, OH^-)_{eq}$ $(N_{amine})_{ax}$[c] |
| | 1.978 | 1.949 | 52.4 | 159.1 | 159.5 | $(N_{amine}, COO^-, 2\times OH^-)_{eq}$ $(O^-_{phe})_{ax}$[b] |
| **VO–sal-*o*-Tyr** | | | | | | |
| II – VOLH | 1.974 | 1.946 | 57.2 | 167.5 | 166.7 | $(O^-_{phe}, N_{amine}, COO^-, OH_2)_{eq}$ $(OH_2$ or $OH_{phe})_{ax}$ |
| III – VOL | 1.974 | 1.946 | 57.2 | 167.5 | 166.7 | $(O^-_{phe}, N_{amine}, COO^-, OH_2)_{eq}$ $(OH_2$ or $O^-_{phe})_{ax}$ |
| | | | | | 165.6 | $(2\times O^-_{phe}, COO^-, OH_2)_{eq}$ $(N_{amine}$ or $OH_2)_{ax}$ |
| | | | | | 168.6 | $(2\times O^-_{phe}, 2\times OH_2)_{eq}$ $(N_{amine}$ or $OH_2$ or $COO^-)_{ax}$ |
| IV – $VOLH_{-1}$ | 1.974 | 1.957 | 56.5 | 167.1 | 166.6 | $(N_{amine}, COO^-, OH_2, OH^-)_{eq}$ $(O^-_{phe})_{ax}$ |
| | | | | | 165.4 | $(O^-_{phe}, COO^-, OH_2, OH^-)_{eq}$ $(N_{amine})_{ax}$ (also possible) |
| **VO–pyr-Tyr** | | | | | | |
| I – VO | 1.977 | 1.936 | 68.5 | 181.5 | 182.6 | $(4\times OH_2)_{eq}$ $(OH_2)_{ax}$ |
| $VOLH_3$ | 1.978 | 1.942 | 61.2 | 172.3 | 173.5 | $(COO^-, N_{amine}, 2\times OH_2)_{eq}$ $(OH_{phe}$ or $OH_2)_{ax}$[b] |
| II – $VOLH_2$[a] | 1.978 | 1.942 | 58.6 | 170.4 | 172.3 | $(O^-_{phe}, COO^-, 2\times OH_2)_{eq}$ $(N_{amine})_{ax}$[b] |
| | 1.978 | 1.952 | 58.6 | 165.9 | 166.7 | $(O^-_{phe}, N_{amine}, COO^-, OH_2)_{eq}$ $(OH_2)_{ax}$[b] |
| III – VOLH[a] | 1.978 | 1.942 | 58.6 | 170.4 | 172.3 | $(O^-_{phe}, COO^-, 2\times OH_2)_{eq}$ $(N_{amine})_{ax}$[b][d] |
| | 1.978 | 1.952 | 58.6 | 165.9 | 166.7 | $(O^-_{phe}, N_{amine}, COO^-, OH_2)_{eq}$ $(OH_2)_{ax}$[b][d] |
| IV – $(VOL)_2H$[a] | 1.981 | 1.940 | 55.8 | 167.6 | 166.7 | $(N_{amine}, COO^-, OH_2, O^-_{phe}$[g]$)_{eq}$ $(O^-_{phe})_{ax}$ |
| | 1.978 | 1.955 | 56.5 | 165.2 | 165.5 | $(O^-_{phe}, COO^-, OH_2, O^-_{phe}$[g]$)_{eq}$ $(N_{amine})_{ax}$ |
| V – $(VOL)_2$[a] | 1.981 | 1.940 | 55.8 | 167.6 | 166.7 | $(N_{amine}, COO^-, OH_2, O^-_{phe}$[g]$)_{eq}$ $(O^-_{phe})_{ax}$ |
| | 1.978 | 1.955 | 56.5 | 165.2 | 165.5 | $(O^-_{phe}, COO^-, OH_2, O^-_{phe}$[g]$)_{eq}$ $(N_{amine})_{ax}$ |
| **VO–pyr-*o*-Tyr** | | | | | | |
| I – VO | 1.977 | 1.936 | 68.7 | 181.4 | 182.6 | $(4\times OH_2)_{eq}$ $(OH_2)_{ax}$ |
| II – $VOLH_2$[a] | 1.978 | 1.942 | 60.2 | 172.7 | 173.5 | $(COO^-, N_{amine}, 2\times OH_2)_{eq}$ $(O^-_{phe}$ or $OH_2)_{ax}$ |
| | 1.978 | 1.949 | 58.3 | 166.6 | 166.7 | $(O^-_{phe}, N_{amine}, COO^-, OH_2)_{eq}$ $(OH_{phe}$ or $OH_2)_{ax}$[e] |
| | | | | | 165.6 | $(2\times O^-_{phe}, COO^-, OH_2)_{eq}$ $(OH_2)_{ax}$[f] |
| III – VOLH | 1.976 | 1.943 | 58.3 | 168.7 | 166.7 | $(O^-_{phe}, N_{amine}, COO^-, OH_2)_{eq}$ $(OH_{phe}$ or $OH_2)_{ax}$[d] |
| | | | | | 165.6 | $(2\times O^-_{phe}, COO^-, OH_2)_{eq}$ $(N_{amine})_{ax}$ |
| IV – VOL | 1.974 | 1.946 | 57.6 | 167.9 | 166.7 | $(O^-_{phe}, N_{amine}, COO^-, OH_2)_{eq}$ $(OH_2$ or $O^-_{phe})_{ax}$ |
| | | | | | 165.5 | $(2\times O^-_{phe}, COO^-, OH_2)_{eq}$ $(N_{amine}$ or $OH_2)_{ax}$ |
| | | | | | 168.6 | $(2\times O^-_{phe}, 2\times OH_2)_{eq}$ $(N_{amine}$ or $OH_2$ or $COO^-)_{ax}$ |
| | | | | | 163.5 | $(O^-_{phe}, N_{amine}, COO^-, OH_2)_{eq}$ $(O^-_{phe}$ or $OH_2)_{ax}$ |
| V – $VOLH_{-1}$ | 1.974 | 1.946 | 56.6 | 167.8 | 165.3 | $(O^-_{phe}, COO^-, OH_2, OH^-)_{eq}$ $(O^-_{phe})_{ax}$ |
| VI – $VOLH_{-2}$ | | ≈ 1.952 | | ≈ 159 | 158.3 | $(O^-_{phe}, COO^-, 2\times OH^-)_{eq}$ $(N_{amine})_{ax}$ |
| | | | | | 159.5 (minor) | $(O^-_{phe}, N_{amine}, 2\times OH^-)_{eq}$ $(COO^-)_{ax}$ |

[a] Probably at least two isomeric species are formed. [b] Phenolate of side chain is protonated. [c] Phenolate of side chain is deprotonated. [d] $N_{pyr}$-deprotonated. [e] $N_{pyr}$-protonated ($N_{pyr}H^+$). [f] $N_{amine}$-protonated ($N_{amine}H^+$). [g] Deprotonated phenolate from the other molecule of the dinuclear species.

$40.1\times10^{-4}$, $A_{z,H2O}$ = $45.7\times10^{-4}$ and $A_{z,OH-}$ = $38.7\times10^{-4}$ cm$^{-1}$. These can be used to establish the most probable binding mode of the complexes formed, but care must be taken as the contributions of the donor groups to the hyperfine coupling may depend on their orientation,[45,46] on the charge of the ligand,[47] and the presence of axial donor groups.[48] Moreover, since several species may coexist in solution and the contributions of each of the donors are not much different, the additivity rule alone cannot provide proof for the binding mode set.

The anisotropic absorption study for **6** shows that between pH 6.0 and 8.5, where the equilibrium VOLH ⇆ VOL takes place, CD spectra (see below) are very similar. Therefore, the ligand coordination sphere should be similar in both species. This is expected since in sal-Tyr the side chain phenolate group is not in a coordinating position, thus this deprotonation step must involve a water molecule coordinated to the vanadium center, and not the phenolate of the Tyr residue (in the ligand the p$K_a$ is 10.93; if the rest of the ligand is coordinated to a metal ion the phenolic OH group of the Tyr moiety usually deprotonates in the pH range 9–10).[49–51] Due to the low solubility of the neutral VOLH, no spectroscopic data was obtained for this species. However, the EPR spectra show the presence of only one species at pH 7.00. According to the spin Hamiltonian parameters obtained for stoichiometry VOL ($A_z$ = $168.6\times10^{-4}$ cm$^{-1}$) we can assign the following equatorial binding set to this species: ($N_{amine}$, $COO^-$, $H_2O$, $OH^-$). Above pH 9.3 the species $VOLH_{-1}$ is observed in which either the deprotonation of the Tyr-OH moiety occurred, or the coordination of another hydroxido group. As the CD data shows a totally different spectral pattern at pH 9.9 and $A_z$ = $159.1\times10^{-4}$ cm$^{-1}$, we consider the latter case as that predominating. Above pH 10, where the quantitatively less clearly described hydroxido vanadium oligomers are formed, the spectra lose intensity (Vis, CD, and EPR), consistent with extensive hydrolysis and the formation of EPR silent vanadium species. Between pH 9.9 and 10.3 the remaining EPR spectra show the presence of two species, which can be assigned to binding isomers, since their ratio

  

does not change (see SI). Table 3 shows the binding modes proposed for each stoichiometry, based on the EPR spectra and spin Hamiltonian parameters obtained.

In **6** coordination of the phenolate of the Tyr residue is possible and several binding modes may compete. The ligand, a racemate, is CD silent. EPR spectra measured for this system (Figure 4) show species with two sets of parameters: one set accounts for $V^{IV}O(OH_2)_5^{2+}$ (**I**) and another accounts for VOLH, VOL, and $VOLH_{-1}$ (**II**–**IV**). The simulation of the EPR spectra at pH 4.52, where VOLH is the major species, suggests tridentate coordination of **2**: $(O_{phenolate}, N_{amine}, COO^-, H_2O)_{eq}$ with $A_z^{est} = 166.7 \times 10^{-4}\,cm^{-1}$. In VOL the *o*-Tyr phenolate group can deprotonate and coordinate, and we propose several plausible binding modes for this stoichiometry with similar $A_z$ values (see Table 3). The coordination of the *o*-Tyr phenolate group equatorially is supported by the stability difference between the $V^{IV}O^{2+}$ complexes of **1** and **2**, therefore the most probable binding mode is $(2 \times O_{phenolate}, COO^-, H_2O)_{eq}(N_{amine})_{ax}$. The formation of $VOLH_{-1}$ is accompanied by a slight decrease in the hyperfine parameter $A_z$ and in absorbance values above pH 9.0. Assuming axially coordinating groups do not affect $A_z$ values, the measured $A_z$, $166.6 \times 10^{-4}\,cm^{-1}$, is relatively high and requires a water molecule to remain in one of the equatorial positions. The data is compatible with binding modes: $(N_{amine}, COO^-, H_2O, OH^-)_{eq}(O_{phenolate})_{ax}$ for $A_z = 166.6 \times 10^{-4}\,cm^{-1}$ and $(O_{phenolate}, COO^-, H_2O, OH^-)_{eq}(N_{amine})_{ax}$ for $A_z = 165.1 \times 10^{-4}\,cm^{-1}$.

For the $V^{IV}O$ systems with **3** and **4** the complex formation starts with $VOLH_2$ below pH 2.0 in both cases. Above pH 3.0 the speciation shows the presence of complexes with stoichiometries VOLH, $(VOL)_2H$, and $(VOL)_2$ in the case of ligand **3**, and VOLH, VOL, and $VOLH_{-1}$, in the case of **4**. The $\log K^*$ values ($V^{IV}O^{2+} + H_4L^+ \leftrightarrows V^{IV}OLH_2 + 2H^+$) of –1.42 and –1.25, for ligands **3** and **4**, respectively, show small differences between the two ligands and indicate similar binding modes. This also indirectly suggests that in the deprotonation of pyr-L-Tyr the $NH^+_{amine}$ deprotonates ($pK_{a3} = 7.67$) before the $NH^+_{pyridine}$ ($pK_{a4} = 9.65$).

The $\log K^*$ values of the process $V^{IV}O^{2+} + H_3L^+ \leftrightarrows V^{IV}OLH + 2H^+$ of –4.78 and –3.19, for **3** and **4**, respectively, show the higher stabilily of the *o*-Tyr derivative in VOLH and indicates that for this stoichiometry the $O_{phenolate}$ (*o*-Tyr) binds to the metal center.

It is clear from the speciation diagrams that all ligands form quite stable complexes with $V^{IV}O^{2+}$ as its hydrolytic products are not formed in measurable concentration at least up to pH 8. The L-Tyr compounds show lower stability than the *o*-Tyr derivatives, and the hydrolytic products of oxidovanadium(IV), $[(V^{IV}O)_2(OH)_5^-]_n$ and $V^{IV}O(OH)_3^-$, have a much higher relative importance in the pH range typical of the formation of these species.

Globally the EPR spectra (see Supporting Information) of the $V^{IV}O$–pyr-Tyr system agree well with the speciation diagram depicted in Figure 3. Namely, at pH 2.01, besides those arising from the aqua complex [$V^{IV}O(H_2O)_5^{2+} \equiv$ VO $\equiv$ **I**], a signal, probably corresponding to $VOLH_2$ (**II**), can already be detected. However, at pH 2.50 a new signal (**III**)

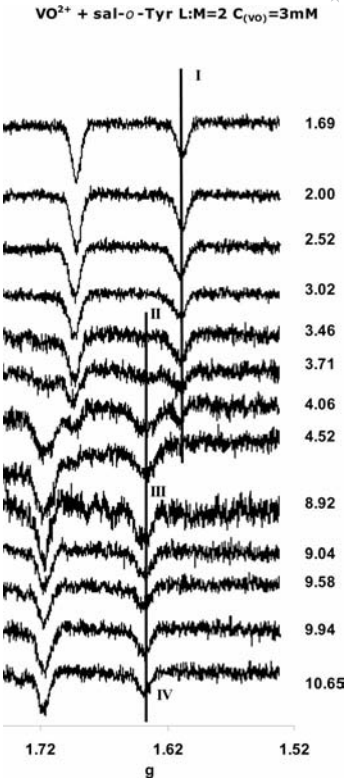


Figure 4. High field region of the EPR spectra of frozen solutions (77 K) containing $V^{IV}O^{2+}$ and sal-*o*-Tyr at several pH values (indicated), with $C_{VO}$ ca. 3 mM and L:M = 2:1. Species labeled **I**–**IV** are assigned in Table 3.

also starts to appear. In the pH range of about 3.0–6.0 these two EPR components coexist, corresponding to $A_z$ values of $170.4 \times 10^{-4}$ and $165.9 \times 10^{-4}\,cm^{-1}$, respectively. Their relative intensity is always the same so they must correspond to isomeric structures of the same stoichiometry. In Table 3 two binding sets are proposed. In these experimental conditions VOLH forms in low amount. We assume it has the same spin-Hamiltonian parameters and the same binding mode as $VOLH_2$, and that deprotonation involves the $N_{pyr}H^+$ group. At pH 6.12 a new species of lower $A_z$ appears and this should correspond to one of the metal ions in the $(VOL)_2H$ species, supposing the deprotonation and coordination of one of the Tyr-$O^-$ groups to the other complex occurs. The dinuclear species has a weak EPR signal, which implies that either the two $V^{IV}O$ centers are far from each other and/or the interaction between their unpaired electrons is not strong. Tyrosyl-dipeptides have been shown to form phenolate-bridged dinuclear complexes with $Cu^{II}$, which were stabilized by hydrophobic stacking interactions between the aromatic rings.[51] A similar kind of dinuclear species might occur in these systems. On increasing the pH further this dinuclear species loses one more proton, which does not dramatically change the EPR spectrum. Above pH ≈ 11, EPR-silent hydrolytic products become important, and the spectra lose intensity.

Although no differences are evident in the EPR behavior of **3** and **4**, the same donor atom arrangements should be

  

assumed in both cases. However, while in the $V^{IV}O$–pyr-Tyr system dinuclear complexes are formed, in the $V^{IV}O$–pyr-*o*-Tyr system our data only indicate the formation of monomeric species. This implies that for the $V^{IV}O$–pyr-*o*-Tyr system the $O_{phenolate}$ from the *o*-Tyr must be involved in binding for the VOLH and VOL stoichiometries.

The CD spectra depicted in Figure 5 show increasing intensity and an isodichroic point at 850 nm between pH 1.65 and 2.50, indicating the formation of a $VOLH_3$ species, which was not detected by pH potentiometry. As the process $VOLH_3 \leftrightarrows VOLH_2$ develops, the band at 560 nm reaches a maximum, that at 770 nm decreases, and that at 935 nm increases in intensity and shifts to higher energy. These changes are in agreement with different binding modes for the two stoichiometries and with an increase in the ligand field. As the processes $VOLH_2 \leftrightarrows VOLH \leftrightarrows (VOL)_2H \leftrightarrows (VOL)_2$ take place as the pH is increased the spectra increase in intensity, and the lower energy band[52] is blue shifted ($\lambda_{max}$ = 810 nm at pH 7.89). Furthermore, relevant modifications take place in the bands observed at 500–600 nm, a positive band at 600 nm is formed and reaches its maximum at pH 7, where VOLH is at maximum concentration. The lower energy band then changes further and its maximum intensity is observed at pH 7.89, where $(VOL)_2H$ is at maximum concentration. From this point forward the intensity of this band decreases; however, at ca. 535 nm the CD intensity increases and reaches a maximum at pH ≈ 9.12, where $(VOL)_2$ is the major species. The increase in the CD signal in Figure 5 (E) at pH 8–10 is compatible with binding sets that include a second $O_{phenolate}$ donor bound to the metal center. Upon further increasing the pH all bands lose intensity and become approximately zero at pH ≈ 11.8. Table 3 includes the proposed binding modes for the different species based on the spectroscopic data.

In the VO–pyr-*o*-Tyr system complex formation starts below pH 2.0. At pH 1.76 the EPR spectrum shows the presence of the aqua complex [$V^{IV}O(H_2O)_5^{2+}$ ≡ VO ≡ **I**] and a minor species, assigned to $VOLH_2$ for which we propose the binding mode: ($COO^-$, $N_{amine}$, $2 \times OH_2)_{eq}$-$(O^-_{pyr-phe})_{ax}$. This coordination mode is present up to pH ≈ 5.5, together with an isomer with an $A_z$ value of

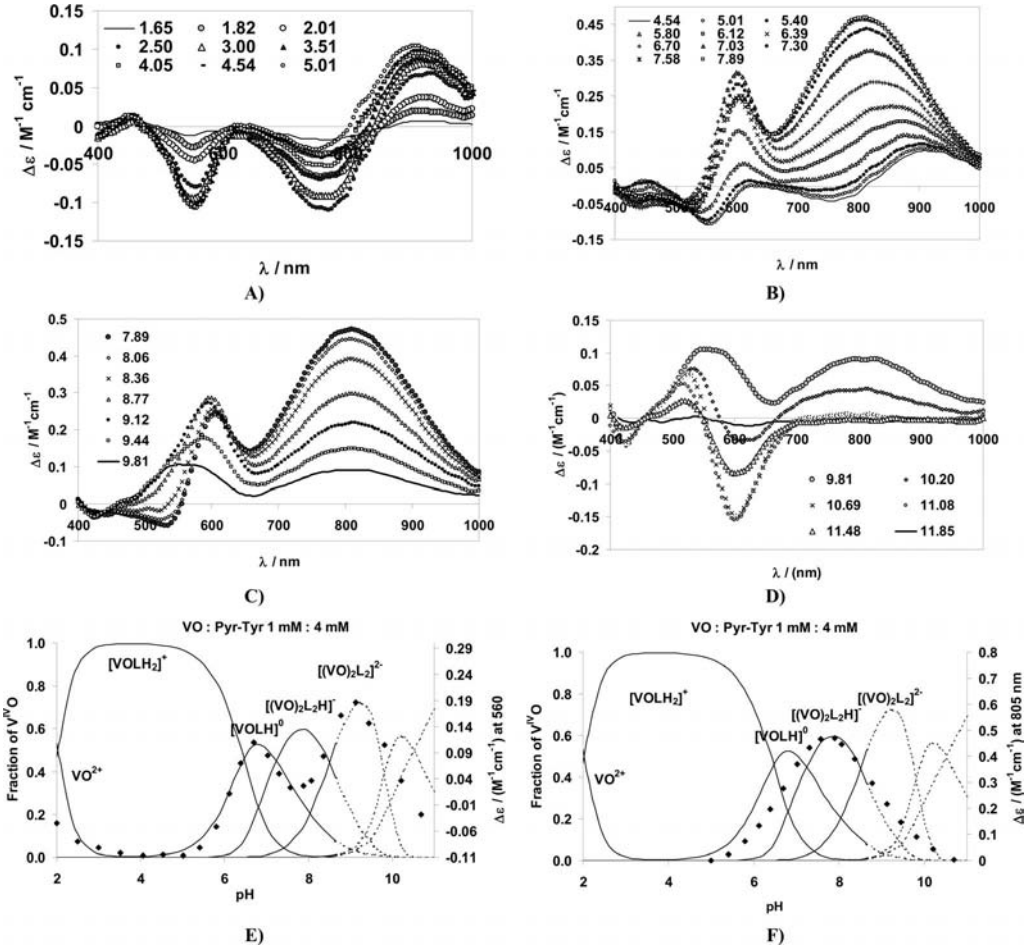


Figure 5. CD spectra recorded for the $V^{IV}O^{2+}$–pyr-L-Tyr system at $C_{VO}$ ca. 3 mM and L:M 4:1. The pH values are indicated. The EPR and Vis spectra for this system are included in the SI. The spectra shown in **A** involve mostly stoichiometries $VOLH_3 \leftrightarrows VOLH_2$, those of **B** and **C** mainly $VOLH_2 \leftrightarrows VOLH \leftrightarrows VOL$ and those of **D** mostly $VOL \leftrightarrows VOLH_{-1}$. **E** and **F** show how the CD data at 545 nm (**E**) and 805 nm (**F**) fit the speciation ($C_{VO}$ = 3 mM and L:M = 4:1). The increase in the CD signal in **E** at pH 8–10 is compatible with binding sets including a second $O_{phenolate}$ donor bound to the metal center.

  

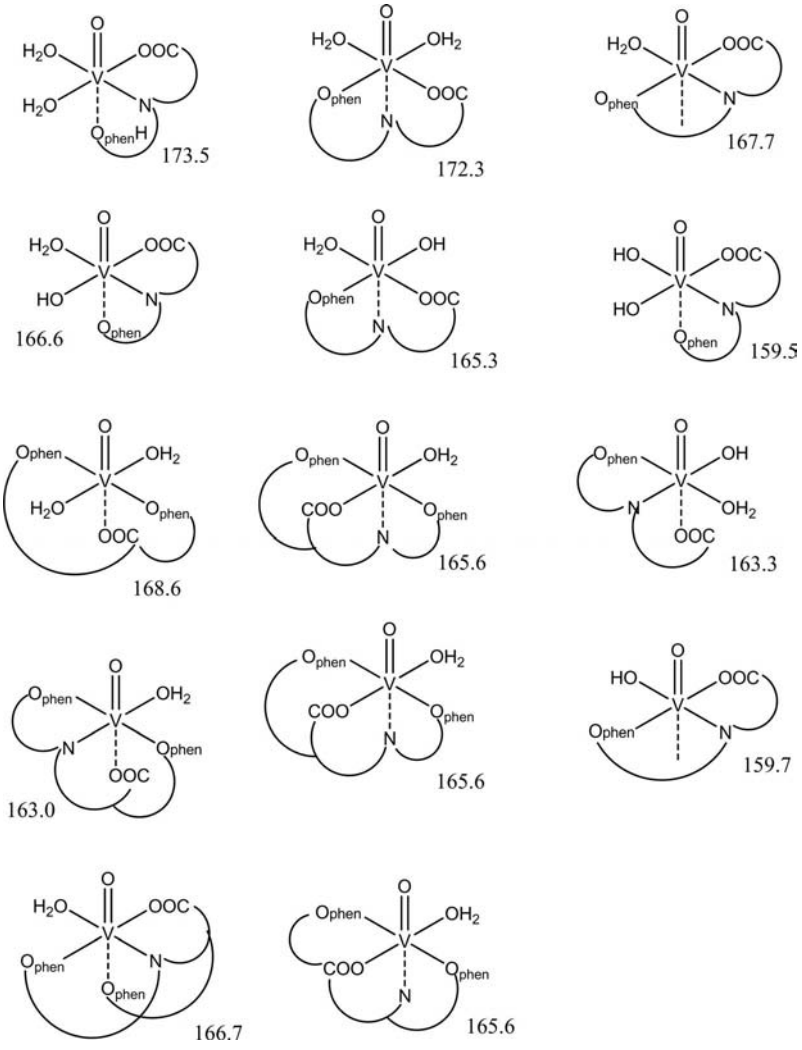


Scheme 3. $A_z^{est}$ values ($\times 10^4$ cm$^{-1}$) for several of the binding modes proposed. It is assumed that axially-bound donor groups do not affect the $A_{z,i}$ of the equatorial groups (this may not be entirely valid).[48]

$166.7 \times 10^{-4}$ cm$^{-1}$ ($COO^-$, $N_{amine}$, $O^-_{pyr-phe}$, $OH_2)_{eq}$. Above pH ≈ 4.0 two processes are most probably happening in parallel (as with $V^V$, vide infra): the deprotonation of the pyridinic nitrogen (which eliminates one of the binding isomers), and the deprotonation and coordination of the *o*-Tyr-OH group. At pH 4.06 a new peak appears with an $A_z$ value of $168.7 \times 10^{-4}$ cm$^{-1}$. Several binding modes are possible (see Table 3), but we suggest the same binding mode for this stoichiometry: ($2\times$ $O^-_{phe}$, $N_{amine}$, $COO^-$, $OH_2)_{eq}$ $(N_{amine})_{ax}$. As the pH is increased only a slight decrease of the hyperfine coupling occurs with the formation of $VOLH_{-1}$, which must involve the deprotonation of a coordinated water molecule. We assign the following binding mode to this stoichiometry: ($O^-_{phe}$, $COO^-$, $OH_2$, $OH^-)_{eq}$ ($O^-_{phe}$ or $OH_2)_{ax}$. At pH 11.44 a new species appears corresponding probably to $VOLH_{-2}$, for which we propose the binding of two $OH^-$ molecules to the vanadium center. Several binding modes may have similar Hamiltonian parameters, and thus we cannot clearly assign one to this species. Some possibilities are included in Table 3 and Scheme 3 depicts several of the binding modes proposed.

## $V^VO_2$ Complexes

To establish the ability of our ligands to interact with $V^VO_2^+$, $^{51}$V NMR spectra were measured with solutions containing ca. 2 mM of vanadate and a L:M of 3:1 at pH ≈ 7.5. To allow the solutions to fully attain equilibrium, spectra were recorded 24 h after the preparation of the samples. The formation of decavanadates was avoided by mixing neutral vanadate solutions (pH ≈ 7.5) with neutral ligand solutions. All ligands showed the ability to form complexes with $V^VO_2$, and Table 4 presents the chemical shift [$\delta$ (ppm)] and the amount of complexes formed. It is clear from the $^{51}$V NMR experiments that the pyridoxal derivatives have a higher affinity for $V^VO_2$ than the salicylaldehyde ligands. For **1** and **2** the chemical shift is found at –526 ppm, in agreement with the formation of $V^VO_2$ complexes with a binding mode involving the tridentate coordination of the ligand through the phenolate, amine, and carboxylate groups.[53] At pH 7.5 the degree of complex formation is low and there is no evidence for the binding of a second $O_{phenolate}$ donor in the case of **2**.

  

Table 4. $^{51}V$ NMR spectroscopic data for the systems studied. The spectra were measured in $H_2O$ containing 5% $D_2O$ at L:M = 3:1 or 6:2 mM 24 h after mixing.

| System | pH | L/M | $\delta(^{51}V)$ [ppm] | % Complex |
|---|---|---|---|---|
| $V^VO_2$–sal-L-Tyr | 7.50 | 3:1 mM | –526 | 10[a] |
| $V^VO_2$–sal-*o*-Tyr | 7.50 | 6:2 mM | –526 | 15[a] |
| $V^VO_2$–pyr-L-Tyr | 7.49 | 6:2 mM | –522, –532 | 10, 90 |
| $V^VO_2$–pyr-*o*-Tyr | 7.09 | 6:2 mM | –490, –534 | 70, 30 |

[a] The other complexes present are inorganic decavanadates. Its presence at these pH values is thermodynamically unfavorable and occurred due to slow equilibration of these solutions.

For **3** and **4** resonances appear at slightly higher field ($\delta \approx -533$ ppm). Ligand **4** shows an additional peak, at –490 ppm, which is the major species at pH ≈ 7, and we propose that in this species there is one more group coordinated, which is the side chain *o*-phenolate. Ligand **3** also presents a very small peak at –522 ppm that we assign to an isomeric complex.

Since pyr-*o*-Tyr showed high affinity for vanadate, potentiometric titrations were carried at different L:$V^VO_2$ ratios to determine the complex formation constants, which are also included in Table 2. For this system, the distribution diagram (Figure 3) includes stoichiometries ($V^VO_2$)-$LH_2$, ($V^VO_2$)LH, and ($V^VO_2$)L. A $^{51}V$ NMR titration was also performed to confirm the potentiometric model and a few of the recorded spectra are included in Figure 6.

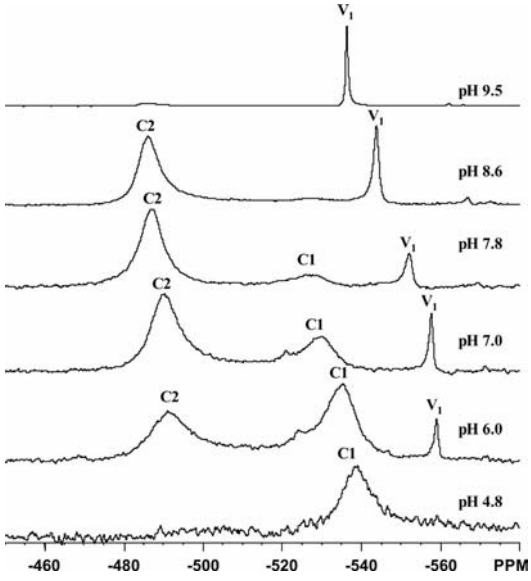


Figure 6. $^{51}V$ NMR spectra obtained at 131.404 MHz and at 25.0 ± 0.5 °C of solutions containing $V^V$ and pyr-*o*-Tyr, $C_V$ = 4 mM and L:M = 2:1 (see text). The pH values are indicated. $V_1$ refers to $HVO_4^{2-}$ and/or $H_2VO_4^-$, the relative amount of $HVO_4^{2-}$ increasing with pH.

The $^{51}V$ NMR peak at ca. –533 ppm (**C1** between –538 ppm and –526 ppm), detected between pH ≈ 4.8 and 8.6 should correspond to two stochiometries $V^VO_2LH_2$ and $V^VO_2LH$, the ligand being probably tridentate and bound by the phenolate, amine, and carboxylate donors. The other peak which appears at ca. –490 ppm (**C2** between –484 ppm and –491 ppm) above pH 6.0, and becomes the major species at pH 7.9, corresponds to $V^VO_2LH$ and $V^VO_2L$. In the latter species the ligand probably binds through two phenolates, the amine, and the carboxylate groups. Both resonances shift as the pH is changed due to the change $V^VO_2LH \rightarrow V^VO_2L$.

## Conclusions

The reduced Schiff bases of salicylaldehyde, pyridoxal, and *o*-vanillin with L-tyrosine and D,L-*o*-tyrosine, as well as $V^{IV}O$(sal-*o*-Tyr) were prepared and characterized in the solid state and in solution. The reduced Schiff base ligands are much less susceptible to hydrolysis than their corresponding Schiff base compounds, which we were not able to isolate in a pure form. They also form much more stable complexes than the corresponding Schiff bases. As expected for a potentially tetradentate ligand as compared to tridentate, the $V^{IV}O$ complexes formed with *o*-Tyr-derived ligands are more stable than those of L-Tyr. In fact, in aqueous solutions containing 1:1 ligand to metal stoichiometry, no $V^{IV}O$-hydrolytic products were detected up to pH 10 in the pyr-*o*-Tyr system, while for the pyr-Tyr system significant amounts of $[(V^{IV}O)_2(OH)_5^-]_n$ form above pH 6.

Mainly 1:1 complexes are formed, the main species having the composition $VOLH_2$ (only for **3** and **4**), VOLH, VOL, and $VOLH_{-1}$. The stability difference between the Tyr and *o*-Tyr derivatives appears only after the binding of the $O_{phenolate}$ donor from the *o*-Tyr moiety, VOL for the Sal and VOLH for the Pyr derivatives. Coordination of the side chain *ortho* phenolic OH occurs to a high extent mainly in the pyr-*o*-tyr complexes, and to a lower extent in the sal-*o*-tyr complexes. A possible explanation for this is the different electronic charge of the ligands, due to the presence of the pyridynic ring in the former ligand, which will increase its solubility/stability in water, particularly in the case of **4**.

## Experimental Section

### Synthesis of Compounds

**sal-L-Tyr (1):** To a suspension of L-Tyr (0.90 g, 5 mmol) in water (25 mL) was added NaOH (4 M) to dissolve the amino acid. To this mixture were added small portions of a solution of salicylaldehyde in MeOH (0.53 mL, 5 mmol in 5 mL); the mixture became yellow, and this color became stronger after the mixing was completed. The solution was cooled with an ice bath, and sodium borohydride (0.37 g, 10 mmol) dissolved in 5 mL of water was slowly added. The solution became colorless and after addition of HCl (until pH ≈ 7.0 was reached) a white solid precipitated, which was collected by filtration, washed with water and MeOH, and dried under vacuum; yield 0.9 g, 60%. $C_{16}H_{17}NO_4 \cdot 1.5H_2O$ (314.34): calcd. C 61.14, H 6.41, N 4.46; found C 61.2, H 6.4, N 4.3. $^1H$ NMR (500 MHz, $D_2O$, pD = 9.60): 2.9 [m, 2 H, Ar–C$H_2$–CH], 3.4 [m, 1 H, C*H*–COOH], 3.9 [dd, 2H Ar–C$H_2$–NH], 6.7 [m, 4 H, $CH_{aromatic}$], 7.1 [m, 4 H, $CH_{aromatic}$]. ESI-MS (MeOH) *m*/*z*: 288.1 ($L^+$, 100%).

**sal-L-Tyr·HCl:** The compound was also obtained as the hydrochloride salt: after the reduction reaction the pH was set to 1–2 by addition of small amounts of concd. aqueous HCl. Then the mix-

  

ture was evaporated until a dry white residue remained. This residue was dissolved in a minimum amount of 2-propanol. The resulting solution was filtered and diethyl ether was added to the filtrate till a white solid precipitated. This was quickly collected by filtration and washed with diethyl ether. Alternatively, the 2-propanol solution was evaporated again and the dry residue was triturated with diethyl ether, collected by filtration, and washed with diethyl ether. The reaction and isolation conditions may allow the formation of the methyl and isopropyl esters of the desired product. The amount of water found in the several syntheses varied from 0 to 2, and the values reported are only an example of some of those found. $C_{16}H_{18}NO_4Cl·1MeOH$ (355.82): calcd. C 57.4, H 6.2, N 3.9; found C 57.1, H 6.2, N 3.7. $^1$H NMR (400 MHz, [D$_6$]DMSO): $\delta$ = 3.02 [dd, 1 H, $^2J_{HH}$ = 14 Hz, $^3J$ = 8.1 Hz, $Ar_{L\text{-}tyr}CH_AH_BCH$], 3.24 [dd, 1 H, $^2J_{HH}$ = 14, $^3J$ = 4.8 Hz, $Ar_{L\text{-}tyr}CH_AH_BCH$], 3.91 [dd, 1 H, $J_1$ = 8.1, $^3J_2$ = 4.8 Hz, $Ar_{L\text{-}tyr}CH_AH_BCH$], 4.1[s, 2 H, $Ar_{sal}CH_2NH_2$], 6.70, 6.72 [d, 2 H, $^3J$ = 8.4 Hz, $Ar_{L\text{-}tyr}$], 6.81 [t, 1 H, $^3J$ = 7.5 Hz, $Ar_{sal}$], 6.98 [d, 1 H, $^3J$ = 8 Hz, $Ar_{sal}$], 7.02, 7.04 [d, 2 H, $^3J$ = 8.4 Hz, $Ar_{L\text{-}tyr}$], 7.2 [t, 1 H, $^3J$ = 8.5 Hz, $Ar_{sal}$], 7.38, 7.4 [d, 1 H, $^3J$ = 7.5 Hz, $Ar_{sal}$]. $^{13}$C NMR (APT) [D$_6$]DMSO: $\delta$ = 34.3 [$Ar_{L\text{-}tyr}CH_2$], 44.4 [$Ar_{sal}CH_2$], 60 [$Ar_{L\text{-}tyr}CH_2CHCOOH$], 115.4 [$Ar_{L\text{-}tyr}$, $(CH)_2COH$], 115.5 [$Ar_{sal}$,$COHCH$], 117.6 [$Ar_{sal}$, $CHC(CH_2)COH$], 119.1 [$Ar_{sal}$,$CH$], 124.8 [$Ar_{L\text{-}tyr}$, $(CH)_2CCH_2$], 130.5 [$Ar_{L\text{-}tyr}$, $(CH)_2CCH_2$], 130.6 [$Ar_{sal}$,$CH$], 132.1 [$Ar_{sal}$, $CHC(CH_2)$], 156.4 [$Ar_{sal}$, $CHC(CH_2)COH$], 156.7 [$Ar_{L\text{-}tyr}$, $(CH_2)$-$COH$], 169.6 [$Ar_{L\text{-}tyr}CH_2CHCOOH$].

**sal-*o*-Tyr (2):** The synthesis was similar to the procedure described for **1** but instead of L-Tyr D,L-*o*-Tyr was used as the amino acid source; yield 0.8 g, 55%. $C_{16}H_{17}NO_4·0.2H_2O$ (290.92): calcd. C 66.06, H 6.03, N 4.81; found C 66.0, H 5.9, N 4.8. $^1$H NMR (500 MHz, $D_2O$, pD = 10.2): $\delta$ = 3.1 [m, 2 H, Ar–$CH_2$–CH], 3.6 [m, 1 H, C$H$–COOH], 4.0 [dd, 2H Ar–C$H_2$–NH], 6.8 [m, 4 H, $CH_{aromatic}$], 7.1 [m, 4 H, $CH_{aromatic}$].

**pyr-L-Tyr (3):** The synthesis was similar to the procedure described for **1** but instead of salicylaldehyde pyridoxal hydrochloride was used as the aldehyde source; yield 1.2 g, 70%. $C_{17}H_{20}N_2O_5·0.8H_2O$ (341.36): calcd. C 58.88, H 6.28, N 8.08; found C 59.0, H 6.3, N 8.0. $^1$H NMR (500 MHz, $D_2O$, pD = 9.4): $\delta$ = 2.2 [s, 3 H, C$H_3$], 3.0 [m, 2 H, Ar–C$H_2$–CH], 3.5 [m, 1 H, C$H$–COOH], 4.1 [dd, 2H Ar–C$H_2$–NH], 4.5 [s, 2H, C$H_2$OH] 6.9 [m, 4H, $CH_{aromatic}$], 7.6 [s, 1 H, $CH_{pyridinic}$].

**pyr-*o*-Tyr (4):** The synthesis was again similar to the procedure described for **1** but instead of salicylaldehyde pyridoxal hydrochloride was used as the aldehyde source and D,L-*o*-Tyr as the amino acid source; yield 1.3 g, 80%. $C_{17}H_{20}N_2O_5·1.1H_2O$ (352.17): calcd. C 57.98, H 6.35, N 7.95; found C 58.0, H 6.3, N 7.8. $^1$H NMR (500 MHz, $D_2O$, pD = 9.5): $\delta$ = 2.3 [s, 3 H, C$H_3$], 3.1 [m, 2 H, Ar–C$H_2$–CH], 3.7 [m, 1 H, C$H$–COOH], 4.1 [dd, 2H Ar–C$H_2$–NH], 4.5 [s, 2 H, C$H_2$OH] 6.9 [m, 4 H, $CH_{aromatic}$], 7.6 [s, 1 H, $CH_{pyridinic}$].

***o*-van-L-Tyr (5):** L-tyrosine (5.00 g, 27.5 mmol) was suspended in methanol (200 mL) and KOH (1.55 g) was added. Stirring was maintained until the solid dissolved, and the resulting mixture was filtered. To the filtrate was added *o*-vanillin (*o*-van, 4.19 g, 27.5 mmol). A yellow color developed and the mixture was left stirring for 24 h. The large amount of yellow precipitate that formed was collected by filtration, dissolved in methanol and the resulting solution was filtered. $NaBH_4$ was added to the filtrate until the yellow color completely disappeared. The pH was adjusted to ca. 2 with HCl and the mixture was evaporated till a dry brownish residue remained. This residue was dissolved in the minimum volume of 2-propanol. The resulting mixture was filtered and diethyl ether was added to the filtrate until a solid precipitated. The resulting cream colored solid was quickly collected by filtration and washed with diethyl ether; yield 1.4 g, 80%. $C_{17}H_{20}NO_5Cl·1.5H_2O$ (380.82): calcd. C 53.6, H 6.1, N 3.7; found C 53.6, H 6.0, N 3.8. In some preparations the solid that precipitated was contaminated with 2-propanol. $^1$H NMR (400 MHz, [D$_4$]MeOH) 3.18 (dd, 1 H, $J_a$ = 14.44 Hz, $J_1$ = 6.69Hz, $Ar_{L\text{-}tyr}CH_aH_bCH$), 3.24 (dd, 1 H, $J_b$ = 14.44 Hz, $J_1$ = 6.16Hz, $Ar_{L\text{-}tyr}CH_aH_bCH$), 3.84 (s, 3 H, C$H_3$O$Ar_{o\text{-}van}$), 4.1 (t, 1 H, $J$ = 6.5 Hz, $Ar_{L\text{-}tyr}CH_2CH$), 4.25 (s, 2 H, $Ar_{o\text{-}van}CHNH_2$), 6.78, 6.8 (d, 2 H, $J$ = 8.47 Hz, $Ar_{L\text{-}tyr}$), 6.81, 6.83, 6.85, 6.87, 6.89 (m, 2 H, $Ar_{o\text{-}van}$), 6.96, 6.98 (dd, 1 H, $J_1$ = 1.54 Hz, $J_2$ = 7.8 Hz, $Ar_{o\text{-}van}$), 7.08, 7.11 (d, 2 H, $J$ = 8.5 Hz, $Ar_{L\text{-}tyr}$). [$^1$H]$^{13}$C NMR (APT) [D$_4$]MeOD; 35.8 ($Ar_{L\text{-}tyr}CH_2$), 47.17 ($Ar_{o\text{-}van}CH_2$), 56.61 ($CH_3OAr_{o\text{-}van}$), 61.29 ($Ar_{L\text{-}tyr}CH_2CHCOOH$), 113.9 ($Ar_{o\text{-}van}$, $CHCHCOMe$), 116.7 [$Ar_{L\text{-}tyr}$, $(CH_2)COH$], 117.7 [$Ar_{o\text{-}van}$, $CHC(CH_2)COH$], 120.9 [$Ar_{o\text{-}van}$, C(CH2)CHCHCHCOMe], 124.1 [$Ar_{o\text{-}van}$, C(CH2)CHCHCHCOMe], 125.5 [$Ar_{L\text{-}tyr}$, $(CH_2)CCH_2$], 131.4 [$Ar_{L\text{-}tyr}$, $(CH_2)CCH_2$], 146.7 [$Ar_{o\text{-}van}$, $CHC(CH_2)COH$], 148.8 ($Ar_{o\text{-}van}$, $CHCHCOMe$), 158.1 [$Ar_{L\text{-}tyr}$, $(CH_2)COH$], 170.4 ($Ar_{L\text{-}tyr}CH_2CHCOOH$).

**VO(sal-*o*-Tyr) (6):** The synthesis was carried at 40 °C under $N_2$. To a solution of **2** (0.29 g, 1 mmol) in water (30 mL) was added NaOH (1 M) until pH 9.5–10 was reached. $V^{IV}OSO_4$ (0.22 g, 0.85 mmol) dissolved in water (10 mL) and sodium acetate trihydrate (0.27 g, 2 mmol) were slowly added. The solution became blue and precipitation of a blue grey solid began. The solution was kept in the refrigerator overnight and then the solid was collected by filtration, washed with water, ethanol, and diethyl ether, and dried under vacuum; yield 0.2 g, 60%. $C_{16}H_{15}NO_5V·1.7H_2O$ (382.86): calcd. C 50.19, H 4.84, N 3.66; found C 50.3, H 4.8, N 3.3.

A few other vanadium-containing complexes were isolated for the other systems, but no satisfactory formulation could be found for these solids.

**pH Metric Measurements:** All measurements were made in aqueous solution. The purity of the ligands was checked pH potentiometrically and the exact concentration of solutions were determined by the Gran method.[54] A stock solution of $V^{IV}O$ was prepared and standardized as reported earlier.[55,56] The $H_3O^+$ concentration in the stock solutions was determined by pH potentiometry. The $V^V$ stock solution was prepared by dissolving $KVO_3$ (Sigma–Aldrich) in an accurately measured volume of a KOH solution of known molarity (ca. 0.20 M), and its $OH^-$ concentration was calculated taking into account the total volume of the $V^V$ stock solution prepared.

All solutions were manipulated in an inert atmosphere (high purity $N_2$ or purified argon). The ionic strength was adjusted to 0.20 M KCl and the temperature was 25.0 ± 0.1 °C. The pH was measured with an Orion 710A precision digital pH meter equipped with an Orion Ross 8103BN type combined glass electrode, calibrated for hydrogen ion concentration.[55] The ionic product of water was p$K_w$ = 13.76.

The protonation constants of the ligands were determined from four titration curves of 4 or 8 mL samples with initial concentrations in the range 0.01 to 0.04 M. Stability constants of the $V^{IV}O$–ligand systems were determined by pH metric titrations of 5, 10, or 20 mL samples. The metal concentrations were in the range 0.0004–0.004 M, and the L:M ratio from 0.5:1 to 8:1. Titrations were normally carried out with KOH solution of known concentration (ca. 0.2 M) under a purified argon atmosphere, from pH 2.0 up to 11.0, unless very extensive hydrolysis, precipitation, or very slow equilibration was detected. Precipitation occurred between pH 4.0 to 9.0 for **1** when the ligand concentration was ca. 4 mM. For ligand **3**

  

slow equilibration or precipitation occurred above pH 6.0. The reproducibility of the titration points included in the evaluation was within 0.005 pH units in the pH range 5–11.

For the determination of the protonation constants corresponding to p$K_{a1}$ (p$K_a$ of the carboxylic acid group), several sets of UV absorption spectra (205–360 nm) with concentrations of ca. 8–$9 \times 10^{-4}$ M were measured in the pH range ca. 0.8 to 12. An individual calibration curve EMF vs. [$H^+$] was established for pH values less than ca. 2, valid for the medium and electrodes. For this purpose a set of HCl solutions was prepared with known $H^+$ concentration, from pH ≈ 0.8 to 2.0, all with an ionic strength of 0.20 M KCl.

The concentration stability constants $\beta_{pqr} = [M_pL_qH_r]/[M]^p[L]^q[H]^r$, where M = $V^{IV}O^{2+}$ or $V^VO_2^+$, were calculated using the PSEQUAD computer program.[57] The formation of the following $V^{IV}O$–hydroxido complexes was taken into account: $[V^{IV}O(OH)]^+$, $[(V^{IV}O)_2(OH)_2]^{2+}$, $[(V^{IV}O)_2(OH)_5]^-$, and $[V^{IV}O(OH)_3]^-$.[52,58,59] As is discussed in ref.[52] the log$\beta$ of $[(V^{IV}O)_2(OH)_5]^-$ and $[V^{IV}O(OH)_3]^-$ are not known accurately; therefore, the calculations for pH > 4 may not be entirely reliable, particularly for systems and experimental conditions where these $V^{IV}O$–hydroxido complexes have significant concentrations. For the $V^V$ systems the stability constants were similarly defined, where M refers to $V^VO_2^+$. The speciation of vanadate into monomeric, dimeric, tetrameric, pentameric, and decameric species was taken into account.[60]

**Physical and Spectroscopic Studies:** IR spectra were recorded with a Jasco FTIR 430 spectrometer. Visible spectra were recorded either with a Hitachi U-2000 or a Perkin–Elmer Lambda 9 UV/Vis/NIR spectrophotometer. The CD spectra were recorded with a JASCO 720 spectropolarimeter, either with a red-sensitive photomultiplier (EXEL-308) suitable for the 400–1000 nm range or with the photomultiplier suitable for the 200–700 nm range. The EPR spectra were recorded at 77 K (on glasses made by freezing solutions in liquid nitrogen) with a Bruker ESP 300E X-band spectrometer. The $^1$H and $^{51}$V NMR spectra were obtained with a Varian Unity-500 NMR spectrometer operating at 499.824 and 131.404 MHz, respectively, using a 5 mm broad band probe and a controlled temperature unit set at 25 ± 1 °C. ESI-MS of methanol or DMSO solutions of the compounds were recorded with a 500-MS Varian Ion Trap Mass Spectrometer in the positive mode (capillary voltage: 80 V; needle voltage: 5 kV; nebulizer gas: nitrogen; nebulizer pressure: 35 psi; drying gas temperature: 350 °C; drying gas pressure: 10 psi; *m*/*z* range recorded: 100–1000).

**Spectrophotometric Measurements**

**UV/Vis and CD Spectroscopy:** All measurements were made on water solutions. The temperature was kept at 25.0 ± 0.3 °C with circulating water. Unless otherwise stated, by visible or CD spectra we mean a representation of $\varepsilon_m$ or $\Delta\varepsilon_m$ values vs. $\lambda$ [$\varepsilon_m$ = absorption/($bC_M$) and $\Delta\varepsilon_m$ = differential absorption/($bC_M$) where $b$ = optical path and $C_M$ = total $V^{IV}$ concentration]. The spectral range covered was normally 350–900 (Vis) and either 240–600 or 400–1000 nm (CD). All measurements and operations of the spectropolarimeter were computer controlled. Normally the spectra were recorded changing the pH with approximately fixed total vanadium and ligand concentrations.

**EPR Spectroscopy:** In the absence of ethylene glycol or DMSO a relatively broad background may be present in the frozen solution EPR spectra, therefore for the measurements with **1** the spectra were run with aqueous solutions containing 5% of DMSO. The $V^{IV}O$ EPR spectra were simulated using a program from Rockenbauer.[40] The EPR spectra help to elucidate which groups coordinate in solution. For the $V^{IV}O$ systems we used the additivity rule to estimate the hyperfine coupling constant $A_z^{est}$.[3,42–44]

**$^1$H and $^{51}$V NMR Spectroscopy:** All samples were prepared at room temperature immediately before acquisition of the NMR spectra. Ligand solutions for the $^1$H NMR pH titrations were prepared in $D_2O$ (99.995%D) weighing the ligand to obtain the desired concentration. The pD values of these solutions were adjusted with DCl and $CO_2$-free NaOD solutions, and measured either using a Crison MicropH 2002 pH-meter with an Ingold 405-M5 combined electrode or a Thermo Orion 420A+ pH meter with a Mettler Toledo U402-M3-S7/200 combined microelectrode (all calibrated at 20 ± 1 °C with standard aqueous buffers at pH 4.0 and 7.0). The final values of pD were determined from pD = pH* + 0.40,[61] where pH* corresponds to the reading of the pH meter.

To obtain $^{51}$V NMR spectra, the solutions containing the $V^V$ complexes were normally prepared by adding the appropriate amounts of the ligand to aqueous sodium vanadate solutions of known concentration and at selected pH values (ca. 8.0) in order to have the desired L:M ratio of 3:1. The initial $V^V$ concentration in the samples was 2 to 5 mM.

For the $^1$H NMR titration of **1**, an 8 mM solution in $D_2O$ was prepared at pD = 0.96 by addition of DCl. Spectra were recorded up to pD = 11.5 by addition of NaOD or DCl. For **2**, an 18 mM solution was prepared in $D_2O$ by addition of NaOD and it was used to measure the spectra by lowering the pD with DCl, but precipitation occurred between pD 9.0 and 4.0. For **3** the concentration was 5 mM and the compound was dissolved at low pD, but even with this concentration precipitation occurred between pH 3.2 and 9.4 and therefore no spectra were measured in this range. A 5 mM solution of **4** was also prepared at pD ≈ 1 in $D_2O$ by addition of DCl. The measurements were performed up to pD = 11.1 by addition of NaOD or DCl.

The $^1$H and $^{51}$V NMR chemical shifts were referenced relative to sodium 3-(trimethylsilyl)-[$D_4$]propionate at 0 ppm and to external neat $VOCl_3$ at 0 ppm, respectively. $^{51}$V NMR acquisition parameters were: 33 kHz spectral width, 30 μs pulse width, 1 s acquisition time, and 10 Hz line broadening. The signal intensities of the NMR resonances were obtained using the line-fitting routine supplied with the NUTS™ PC-based NMR spectral analysis program.[62]

**X-ray Crystal Structure Determination of 3:** Three-dimensional X-ray data for **3** was collected on a Siemens Smart 1000 CCD diffractometer by the ϕ–ω scan method. Data was collected at room temperature. Reflections were measured from a hemisphere of data collected of frames each covering 0.3 ° in ω. Of the 10960 reflections measured, all of which were corrected for Lorentz and polarization effects and for absorption by multiscan methods based on symmetry-equivalent and repeated reflections, 3128 independent reflections exceeded the significance level ($|F|/\sigma|F|$) > 4.0. Complex scattering factors were taken from the program package SHELXTL.[63] The structures were solved by direct methods and refined by full-matrix least-squares methods on $F^2$. Non-hydrogen atoms were refined with anisotropic thermal parameters in all cases. Hydrogen atoms were included in calculated positions and refined by using a riding mode for all the atoms except for N(1), N(2), C(3), C(8), C(9), C(11), C(13), C(14), C(16), C(17), and O(5), which were freely refined. Refinement was performed with allowance for thermal anisotropy of all non-hydrogen atoms. The crystal presents two disorders in C(1) and O(1) on the $CH_2OH$ group and in C(5) on the $CH_3$ group. These disorders have been solved and two atomic sites for each atom have been observed and refined with anisotropic atomic displacement parameters. The site occupancy factors were 0.65905 for C(1A) and O(1A), and 0.46519 for C(5A).

  

The crystal used for analysis was a merohedral twin, as indicated the Flack parameter of 0.7(13) (1252 Friedel pairs).[64,65] A final difference Fourier map showed no residual density outside: 0.405, –0.262 e Å$^{-3}$. Crystal data and structure refinement parameters are collected in Table 5. The structure was solved using the SHELXS[66] Program for Crystal Structure Determination and refined with SHELXL[67] Program for Crystal Structure Refinement.

Table 5. Crystal data and structure refinement parameters for **3**.[a]

| | pyr-L-Tyr (**3**) |
|---|---|
| Formula | $C_{17}H_{20}N_2O_5$ |
| $M_r$ | 332.35 |
| $T$ [K] | 298(2) |
| Crystal system | orthorhombic |
| Space group | $P2_12_12_1$ |
| $a$ [Å] | 8.6613(5) |
| $b$ [Å] | 12.2976(7) |
| $c$ [Å] | 15.9747(10) |
| $V$ [Å$^3$] | 1701.52(17) |
| $F$(000) | 704 |
| $Z$ | 4 |
| $D_c$ [g cm$^{-3}$] | 1.297 |
| $\mu$ [mm$^{-1}$] | 0.096 |
| $R_{int}$ | 0.0265 |
| Reflections measured | 10960 |
| Independent reflections[b] | 3128 |
| Goodness-of-fit on $F^2$ | 1.024 |
| $R_1$[c] | 0.0482 |
| $wR_2$ (all data)[c] | 0.1214 |

[a] The structures were solved using the SHELXS Program for Crystal Structure Determination and refined with SHELXL (program for crystal structure refinement).[66,67] [b] $I > 2\sigma(I)$. [c] $R_1 = \Sigma||F_o| - |F_c||/\Sigma|F_o|$, $wR_2 = \{\Sigma[w(||F_o|^2 - |F_c|^2|)^2]/\Sigma[w(F_o^4)]\}^{1/2}$.

CCDC-791752 contains the supplementary crystallographic data for this paper. These data can be obtained free of charge from the Cambridge Crystallographic Data Centre via www.ccdc.cam.ac.uk/data_request/cif.

**Supporting Information** (see footnote on the first page of this article): Figure SI1: hydrogen bonds in the structure of compound **3**, figure SI2: IR spectra of the compounds, figure SI3: study of the protonation processes of the compounds, figure SI4: spectroscopic studies of the $V^{IV}O$ systems, figure SI5: deprotonation sequences for **1** and **3**.

## Acknowledgments

The authors are grateful to the Hungarian National Research Fund, Országos Tudományos Kutatási Alapprogramok (OTKA) ( (NI77833), the Hungarian Academy of Sciences, the Fundo Europeu para o Desenvolvimento Regional (FEDER), the Fundação para a Ciência e Tecnologia (FCT), the Hungarian–Portuguese Intergovernmental S&T Co-operation Programme for 2008–2009, and the University of La Coruña and the Spanish–Portuguese Bilateral Programme (Acção Integrada E-56/05, Acción Integrada HP2004-0074). The authors also wish to thank the Portuguese NMR Network (IST-UTL Center), the Portuguese National Mass Spectroscopy Network (RNEM, IST-UTL Center) for providing access to the NMR and MS facilities, and Dr. M. M. C. A. Castro for the help in recording several $^{51}V$ NMR spectra.

[1] V. L. Pecoraro, C. A. Slebodnick, B. Hamstra, in: *Vanadium Compounds: Chemistry, Biochemistry and Therapeutic Applications* (Eds.: A. S. Tracey, D. C. Crans), ACS, Washington, **1998**, p. 157–167.
[2] R. R. Eady, *Coord. Chem. Rev.* **2003**, *237*, 23–30.
[3] D. Rehder, in: *Bioinorganic Vanadium Chemistry*, John Wiley & Sons, New York, **2008**, and references cited therein.
[4] K. H. Thompson, J. H. McNeill, C. Orvig, *Chem. Rev.* **1999**, *99*, 2561–2571.
[5] J. T. Thompson, C. Orvig, *J. Chem. Soc., Dalton Trans.* **2000**, 2885–2892.
[6] C. Orvig, K. H. Thompson, *Coord. Chem. Rev.* **2001**, *219–221*, 1033–1053.
[7] H. Sakurai, *Chem. Rec.* **2002**, *2*, 237–248.
[8] H. Sakurai, H. Yasui, Y. Adachi, *Expert Opin. Invest. Drugs* **2003**, *12*, 1189–1203.
[9] K. H. Thompson, J. Lichter, C. Lebel, M. C. Scaife, J. H. McNeill, C. Orvig, *J. Inorg. Biochem.* **2009**, *103*, 554–558.
[10] M. W. Makinen, M. J. Brady, *J. Biol. Chem.* **2002**, *277*, 12215–12220.
[11] A. E. Evangelou, *Crit. Rev. Oncol. Hematol.* **2002**, *42*, 249–265.
[12] P. Koepf-Maier, H. Z. Kopf, *Z. Naturforsch., Teil B* **1979**, *34*, 805–807.
[13] A. Papaioannou, M. Manos, S. Karkabounas, R. Liasko, A. M. Evangelou, I. Correia, V. Kalfakakou, J. Costa Pessoa, T. Kabanos, *J. Inorg. Biochem.* **2004**, *98*, 959–968.
[14] Y. Fu, Q. Wang, X. G. Yang, X. D. Yang, K. Wang, *J. Biol. Inorg. Chem.* **2008**, *13*, 1001–1009.
[15] D. C. Crans, J. J. Smee, E. Gaidamaukas, L. Yang, *Chem. Rev.* **2004**, *104*, 849–902, and references cited therein.
[16] K. G. Peters, M. G. Davis, B. W. Howards, M. Pokross, V. Rastogi, C. Diven, K. D. Greis, E. Eby-Wilkens, M. Maier, A. Evdokimov, S. Soper, F. Genbauffe, *J. Inorg. Biochem.* **2003**, *96*, 321–330, and references cited therein.
[17] E. Tsiani, I. G. Fantus, *Trends Endocrinol. Metab.* **1997**, *8*, 51–58.
[18] B. I. Posner, R. Faure, J. W. Burgess, A. P. Bevand, D. Lachance, G. Zhang-Sun, I. G. Fantus, J. B. Ng, D. A. Hall, B. Soo Lum, A. Shaver, *J. Biol. Chem.* **2009**, *269*, 4696–4604.
[19] A. Butler, H. Eckert, *J. Am. Chem. Soc.* **1989**, *111*, 2802–2809.
[20] T. Kiss, T. Jakusch, D. Hollender, A. Dornyei, E. A. Enyedy, J. Costa Pessoa, H. Sakurai, A. Sanz-Medel, *Coord. Chem. Rev.* **2008**, *252*, 1153–1162.
[21] T. Jakusch, D. Hollender, E. A. Enyedy, C. S. Gonzalez, M. Montes-Bayon, A. Sanz-Medel, J. Costa Pessoa, I. Tomaz, T. Kiss, *Dalton Trans.* **2009**, 2428–2437.
[22] D. Sanna, G. Micera, E. Garribba, *Inorg. Chem.* **2009**, *48*, 5747–5757.
[23] D. Sanna, E. Garribba, G. Micera, *J. Inorg. Biochem.* **2009**, *103*, 648–655.
[24] D. R. Davies, H. Interthal, J. J. Champoux, G. J. Wim, W. G. J. Hol, *Chem. Biol.* **2009**, *10*, 139–147.
[25] a) D. Rehder, H. Holst, W. Priebsch, H. Vilter, *J. Inorg. Biochem.* **1991**, *41*, 171–185b) M. Ebel, D. Rehder, *Inorg. Chem.* **2006**, *45*, 7083–7090.
[26] I. Cavaco, J. Costa Pessoa, D. Costa, M. T. Duarte, R. D. Gillard, P. M. Matias, *J. Chem. Soc., Dalton Trans.* **1994**, 149–157.
[27] J. Costa Pessoa, I. Cavaco, I. Correia, M. T. Duarte, R. D. Gillard, R. T. Henriques, F. J. Higes, C. Madeira, I. Tomaz, *Inorg. Chim. Acta* **1999**, *293*, 1–11.
[28] S. Dutta, S. Mondal, A. Chakravorty, *Polyhedron* **1995**, *14*, 1163–1168.
[29] I. Cavaco, J. Costa Pessoa, M. T. Duarte, R. T. Henriques, P. M. Matias, R. D. Gillard, *J. Chem. Soc., Dalton Trans.* **1996**, 1989–1996.
[30] R. Fulwood, H. Schmidt, D. Rehder, *J. Chem. Soc., Chem. Commun.* **1995**, 1443–1444.
[31] I. Correia, J. Costa Pessoa, M. T. Duarte, R. T. Henriques, M. F. M. Piedade, L. F. Veiros, T. Jakusch, A. Dornyei, T. Kiss, M. M. C. A. Castro, C. F. G. C. Geraldes, F. Avecilla, *Chem. Eur. J.* **2004**, *10*, 2301–2317.

  

[32] L. P. Koh, J. O. Ranford, W. T. Robinson, J. O. Svensson, A. L. C. Tan, D. Wu, *Inorg. Chem.* **1996**, *35*, 6466–6472.
[33] M. R. Maurya, S. Khurana, D. Rehder, *Transition Met. Chem.* **2003**, *28*, 511–517.
[34] J. Costa Pessoa, I. Correia, T. Kiss, T. Jakusch, M. M. C. A. Castro, C. F. G. C. Geraldes, *J. Chem. Soc., Dalton Trans.* **2002**, 4440–4450.
[35] J. Costa Pessoa, S. Marcão, I. Correia, G. Goncalves, A. Dornyei, T. Kiss, T. Jakusch, I. Tomaz, M. M. C. A. Castro, C. F. G. C. Geraldes, F. Avecilla, *Eur. J. Inorg. Chem.* **2006**, 3595–3606.
[36] I. Correia, J. Costa Pessoa, M. T. Duarte, M. F. M. Piedade, T. Jakusch, T. Kiss, M. M. C. A. Castro, C. F. G. C. Geraldes, F. Avecilla, *Eur. J. Inorg. Chem.* **2005**, 732–744.
[37] P. Adão, J. Costa Pessoa, R. T. Henriques, M. L. Kuznetsov, F. Avecilla, M. R. Maurya, U. Kumar, I. Correia, *Inorg. Chem.* **2009**, *48*, 3542–3561.
[38] G. Socrates, *Infrared and Raman Characteristic Group Frequencies. Tables and Charts*, **2001**, John Wiley & Sons, Chichester, vol. 3, p. 108–113.
[39] E. Garribba, G. Micera, D. Sanna, *Inorg. Chim. Acta* **2006**, *359*, 4470–4476.
[40] A. Rockenbauer, L. Korecz, *Appl. Magn. Reson.* **1996**, *10*, 29–43.
[41] D. E. Metzler, E. E. Snell, *J. Am. Chem. Soc.* **1955**, *77*, 2431–2437.
[42] K. Wüthrich, *Helv. Chim. Acta* **1965**, *48*, 1012–1017.
[43] N. D. Chasteen, in: *Biological Magnetic Resonance* **1981**, vol. 3, Plenum, New York, p. 53–119.
[44] T. Jakusch, P. Buglyó, I. Tomaz, J. Costa Pessoa, *Inorg. Chim. Acta* **2002**, *339*, 119–128.
[45] T. S. Smith, C. A. Root, J. W. Kampf, P. G. Rasmussen, V. L. Pecoraro, *J. Am. Chem. Soc.* **2000**, *122*, 767–775.
[46] G. Micera, V. L. Pecoraro, E. Garribba, *Inorg. Chem.* **2009**, *48*, 5790–5796.
[47] A. J. Tasiopoulos, A. N. Troganis, A. E. Evangelou, C. P. Raptopoulou, A. Terzis, Y. Deligiannakis, T. Kabanos, *Chem. Eur. J.* **1999**, *5*, 910–921.
[48] S. Gorelsky, G. Micera, E. Garribba, *Chem. Eur. J.* **2010**, *16*, 8167–8180.
[49] L. Pettit, J. Swash, *J. Chem. Soc., Dalton Trans.* **1982**, 485–486.
[50] T. Kiss, A. Gergely, *J. Chem. Soc., Dalton Trans.* **1984**, 1951–1957.
[51] T. Kiss, Z. Szucs, *J. Chem. Soc., Dalton Trans.* **1986**, 2443–2447.
[52] L. F. Vilas Boas, J. Costa Pessoa, in: *Comprehensive Coordination Chemistry* (Eds.: G. Wilkinson, R. D. Gillard, J. A. McCleverty), **1987**, Pergamon Press, Oxford, p. 453–583.
[53] D. Rehder, C. Weideman, A. Duch, W. Priebsch, *Inorg. Chem.* **1988**, *27*, 584–587.
[54] G. Gran, *Acta Chem. Scand.* **1950**, *4*, 559–575.
[55] J. Costa Pessoa, T. Gajda, R. D. Gillard, T. Kiss, S. M. Luz, J. J. G. Moura, I. Tomaz, J. P. Telo, I. Torok, *J. Chem. Soc., Dalton Trans.* **1998**, 3587–3600.
[56] I. Nagypal, I. Fábián, *Inorg. Chim. Acta* **1982**, *61*, 109–113.
[57] L. Zekany, I. Nagypal, in: *Computational Methods for the Determination of Stability Constants*, **1985**, Plenum, New York.
[58] A. Komura, M. Hayashi, H. Imanaga, *Bull. Chem. Soc. Jpn.* **1977**, *50*, 2927–2931.
[59] R. P. Henry, P. C. H. Mitchell, J. E. Prue, *J. Chem. Soc., Dalton Trans.* **1973**, 1156–1159.
[60] L. Pettersson, B. Hedman, I. Andersson, N. Ingri, *Chim. Scripta* **1983**, *22*, 254–264.
[61] P. K. Glasoe, F. A. Long, *J. Phys. Chem.* **1960**, *64*, 188–190.
[62] *NUTS-NMR Data Processing Software*, Acorn NMR Inc., Livermore, CA, USA, **1999**.
[63] G. M. Sheldrick, *SHELXTL*, University of Göttingen, Germany, **1997**.
[64] H. D. Flack, *Acta Crystallogr., Sect. A* **1983**, *39*, 876–881.
[65] G. Bernardinelli, H. D. Flack, *Acta Crystallogr., Sect. A* **1985**, *41*, 500–511.
[66] G. M. Sheldrick, *SHELXS-97*, University of Göttingen, Germany, **1997**.
[67] G. M. Sheldrick, *SHELXL-97: An Integrated System for Solving and Refining Crystal Structures from Diffraction Data* (rev. 5.1), University of Göttingen, Germany, **1997**.

Received: September 7, 2010
Published Online: January 10, 2011

  